NASA Conference Publication 2453

Joint University Program for Air Transportation Research—1985

Proceedings of a conference held in Atlantic City, New Jersey January 30, 1986

NASA

NASA Conference Publication 2453

Joint University Program for Air Transportation Research—1985

Compiled by
Frederick R. Morrell
Langley Research Center
Hampton, Virginia

Proceedings of a conference sponsored by the National Aeronautics and Space Administration and the Federal Aviation Administration and held in Atlantic City, New Jersey
January 30, 1986

National Aeronautics
and Space Administration

Scientific and Technical Information Office

1987

PREFACE

The Joint University Program for Air Transportation Research is a coordinated set of three grants jointly sponsored by NASA Langley Research Center and the Federal Aviation Administration, one each with Massachusetts Institute of Technology (NGL-22-009-640), Ohio University (NGR-36-009-017), and Princeton University (NGL-31-001-252), to support the training of students for the air transportation system. These grants, initiated in 1971, encourage the development of innovative curriculums and support the establishment of graduate and undergraduate research assistantships and internships.

An important feature of this program is the quarterly review, one held at each of the schools and a fourth at a NASA or FAA facility. This latter review for 1985 was held at the Federal Aviation Administration Technical Center, Atlantic City, New Jersey, January 30, 1986. At these reviews the program participants, both graduate and undergraduate, have an opportunity to present their research activities to their peers, professors, and invited guests from government and industry.

This conference publication represents the sixth in a series of yearly summaries of the activities of the program (the 1984 summary appears in NASA CP-2452). The majority of the material is the effort of the students supported by the grants.

Three types of contributions are included. Completed works are represented by full technical papers. Research reported in the open literature (for example, theses or journal articles) is presented in an annotated bibliography. Status reports of ongoing research are represented by copies of viewgraphs augmented with a brief descriptive text.

Use of trade names or manufacturers in this report does not constitute an official endorsement of such products or manufacturers, either expressed or implied, by the National Aeronautics and Space Administration or the Federal Aviation Administration.

Frederick R. Morrell
NASA Langley Research Center

CONTENTS

MASSACHUSETTS INSTITUTE OF TECHNOLOGY

INVESTIGATION OF AIR TRANSPORTATION TECHNOLOGY AT MASSACHUSETTS INSTITUTE OF TECHNOLOGY, 1985

Robert W. Simpson
Flight Transportation Laboratory
Massachusetts Institute of Technology
Cambridge, Massachusetts

INTRODUCTORY REMARKS AND OVERVIEW

There were two areas of research sponsored under the Joint University Program during 1985. The first is the investigation into runway approach flying with Loran-C, involving flight tests in a Grumman Tiger. The second is a series of research topics in the development of experimental validation methodologies to support aircraft icing analysis, which also has involved flight tests in the Twin Otter Icing Research Aircraft at NASA Lewis Research Center.

1. RUNWAY APPROACH FLYING USING LORAN-C

This project is aimed at exploring the capabilities of Loran-C to provide cross-pointer approach displays for the general-aviation pilot which can be used to fly approaches to any runway located in good Loran-C signal coverage. Cross-track and vertical deviations from the runway centerline are derived from a Loran-C local coordinate frame centered on the runway touchdown point, thus avoiding any transformation into geodetic latitude and longitude and allowing an easy update of current time differences at the airport, as recorded from a monitor at the airport. Vertical deviations are derived from Loran-C estimates of range to touchdown, given the glide slope, and a digitized electronic pressure altimeter.

The first phase of research work was completed by John K. Einhorn, resulting in his S.M. thesis entitled, "Probabilistic Modeling of Loran-C from Non-Precision Approaches." This phase formulated a mathematical model of expected position errors for a Loran-C approach at a given runway located relative to the Loran-C transmitter. From this position, error ellipses were generated, corresponding to two time difference correction schemes. The first involved relaying corrections to the pilot just before he initiated the approach, and the other involved publishing corrections on the instrument approach plates every few months. It was found that both schemes provided errors well within the FAA AC 90-45A accuracy standards, and that the first scheme was a significant improvement over the latter.

Flight tests in Phase I were conducted in the Grumman Tiger, carrying an equipment test bed designed to take data from a Loran-C receiver and instrument landing system (ILS) localizer receiver. These tests were flown at four different airports within the 9960 Northeast chain of domestic Loran-C coverage: Hanscom Field at Bedford, Massachusetts; Groton, Connecticut; Newport, Rhode Island; and Bar Harbor, Maine. Differences from the ILS localizer averaged 0.65° (equivalent to 97 feet at runway threshold or 270 feet at the outer marker of the approach), and the Loran-C appeared to provide very good localizer tracking. It was concluded that Loran-C is a suitable system for non-precision approaches, and that time-difference corrections made every eight weeks in the instrument approach plates will produce acceptable errors.

The second phase of the Loran-C research is continuing with the work by Norry Dogan. It is exploring the possibilities of pseudo-precision approach flying, using an altimeter-aided display system to provide both cross-track and vertical deviations from the approach centerline and glidepath. An electronic approach display system has been built, and an interface has been provided with a King Radio KEA-346 altimeter. The tracking dynamics of the Loran-C receiver have been tested in ground vehicle trials and can be modeled as a second-order system with a damping ratio around 0.5 and a time constant of approximately 18 seconds. Preliminary flight tests have been flown at Hanscom Field, Bedford, Massachusetts, showing that Loran-C approaches can be flown using an approach display based on Loran-C. However, further tests are contemplated to eliminate various deficiencies found in the operation of the system.

A highlight of the year was the announcement that the W. E. Jackson Award for the best student thesis had been awarded to John Einhorn by the Radio Technical Commission for Aeronautics. It is available as MIT FTL Report R85-5 (Reference 1).

2. EXPERIMENTAL METHODOLOGIES TO SUPPORT AIRCRAFT ICING ANALYSIS

Research efforts in this area stem from original work sponsored by this program on the demonstration of the use of ultrasonic transducers to measure accurately the thickness of a layer of ice on a surface. As described in Reference 2, an ultrasonic pulse is emitted from the transducer and reflects off the ice/air interface to be detected by the transducer acting as a receiver. Since experiments have shown that the speed of sound in various types of aircraft ice is constant, the time lapse can be used to determine ice-layer thickness above the transducer imbedded in the surface. Accuracies greater than a millimeter are possible, and ice accretion rates over time can be determined even if they vary. It is possible to identify whether there is a layer of water present at the ice/air interface.

After tests in the Icing Research Tunnel at NASA Lewis Research Center which measured ice accretion on a circular cylinder at light and heavy, wet, dry, rime or glaze conditions, similar cylinder flight tests onboard the Twin Otter Icing Research Aircraft were conducted in real icing conditions. The increased accuracy allowed measurement of icing rates in terms of mm/min (instead of inches/hour from other means) and allowed a good correlation to be established with the time variation in liquid water content of the icing cloud, as measured by onboard instrumentation. While development of improved ultasonic detection systems continued during the year in the form of an array of small transducers to be mounted around a cylinder or leading-edge glove mounted on the aircraft wing and a high-speed digital data acquisition system, the real objectives of the research project are to develop a model which explains the role of various parameters in aircraft ice accretion.

A simple steady-state heat-transfer model was used to validate the heat-transfer data used by Lewis Research Center. Accretion rates in wet and dry conditions at various cloud temperatures were consistent with experimental results. Small-scale air turbulence in the tunnel was used to show that turbulence was significantly lower in real flight conditions. The role of sublimation was identified. It is important as a heat-transfer mechanism, and the decrease in ice thickness in clear air due to sublimation was shown to be less than 1 mm per hour.

Further Twin Otter wing glove flight tests are being planned to obtain time and space ice-growth data. These flight test data will be compared with analytical prediction for computational models and scaling analysis. In addition, the instrumented glove will be tested in the Icing Research Tunnel.

These data sets will provide a unique opportunity for the direct comparison of the various icing analysis and certification tools currently in use.

ANNOTATED REFERENCES

1. Einhorn, John K., "Probabilistic Modeling of Loran-C for Non-Precision Approaches," MIT FTL Report R85-5, Flight Transportation Laboratory, MIT, Cambridge, MA 02139, 1985.

   This report creates a model for expected position errors at a runway approach located in a given Loran-C triad. Expected position-error ellipses were generated for two correction schemes for Loran time differences. The "update each approach" scheme was shown to be significantly better than the "publish approach plates every eight weeks" scheme, although the latter was well within the accuracy standards called for by FAA AC90-45A for non-precision approaches. Flight tests at four different airports in the 9960 Northeast USA Loran-C chain demonstrated the flyability of the Loran-C localizer path, and showed an average error of 0.65 degrees between ILS localizer and Loran-C data.

2. Hansman, R. John, Jr. and Kirby, Mark S., "Measurement of Ice Accretion Using Ultrasonic Pulse-Echo Techniques," J. Aircraft, vol. 22, No. 6, June 1985.

   Results of tests to measure ice thickness using ultrasonic pulse-echo techniques are presented. Tests conducted on simulated glaze ice, rime ice, and ice crystals are described. Additional tests on glaze and rime ice samples formed in the NASA Lewis Icing Research Tunnel are also described. The speed of propagation of the ultrasonic wave used for pulse-echo thickness measurement is found to be insensitive to the type of ice structure, and is determined to be 3.8 mm/μs. An accuracy of ±0.5 mm is achieved for ice thickness measurements using this technique.

ANNOTATED BIBLIOGRAPHY

1. Hansman, R. John, Jr., "Measurement of Individual Hydrometeor Absorption Cross Sections Utilizing Microwave Cavity Perturbation Techniques," J. of Atmospheric and Oceanic Technology, vol. 1, No. 4, December 1984.

   A technique for measurement of individual hydrometeor absorption cross sections is presented. Cross sections are inferred by inserting the hydrometeor into a high Q resonant cavity and measuring the Q perturbation. Tests were conducted in a 10.64 GHz, TM_{010} cavity. Absorption cross sections were measured at room temperature for 0.5 to 2.0 mm water drops, and were found to agree with the Rayleigh theory. Cross sections were also measured as a function of temperature, and from these the dielectric loss term Im(-K) was inferred for supercooled water down to -17°C.

2. Hansman, R. John, Jr., "Droplet Size Distribution Effects on Aircraft Ice Accretion," J. Aircraft, vol. 22, No. 6, June 1985.

The impinging mass flux distribution which determines aircraft ice accretion rate is shown to be related to the atmospheric droplet size distribution through the droplet collection efficiency of the body. Collection efficiency is studied by means of a two-dimensional droplet-trajectory code which includes the effect of nonspherical droplet shape due to hydrodynamic deformation. The simulation was found to agree with wind tunnel photographic studies of droplet kinematics. The results of the simulation are used to generate impinging mass flux distributions for typical cloud and precipitation size distributions. The impinging mass approach is also used to determine relative icing rates from several supercooled cloud characterizations including the intermittent maximum icing envelope of Federal Aviation Regulation, Part 25.

N87-27598

EXPERIMENTAL METHODOLOGIES TO SUPPORT AIRCRAFT ICING ANALYSIS

R. John Hansman, Jr. and Mark S. Kirby
Massachusetts Institute of Technology
Cambridge, Massachusetts

This figure shows typical ultrasonic echo signals for dry "rime" ice growth.

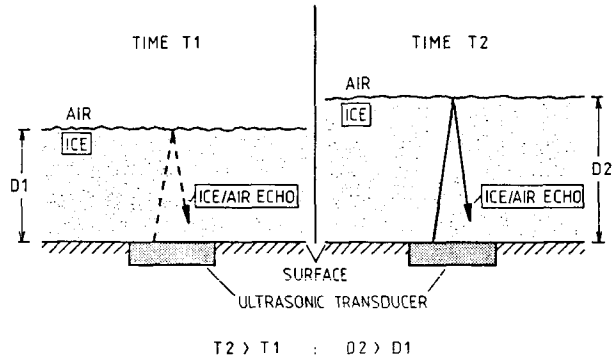

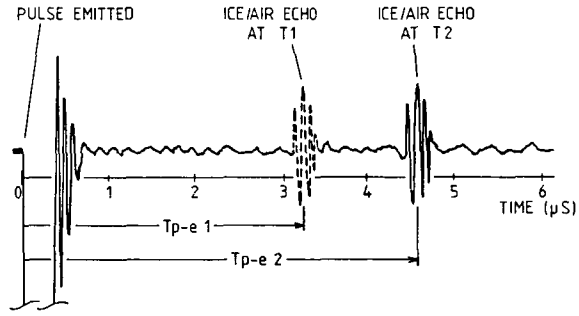

This figure shows typical ultrasonic echo signals for wet "glaze" ice growth. The presence of surface water is identified by multiple echoes in the water layer which have a distinctive frequency behavior resulting from changes in the water layer thickness due to surface waves and droplet impact.

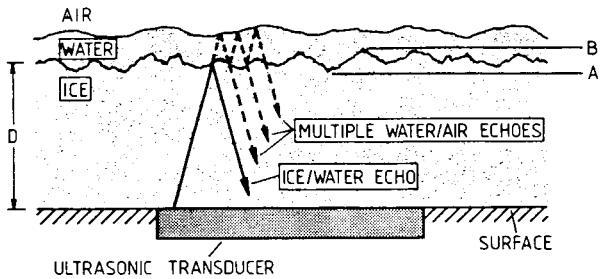

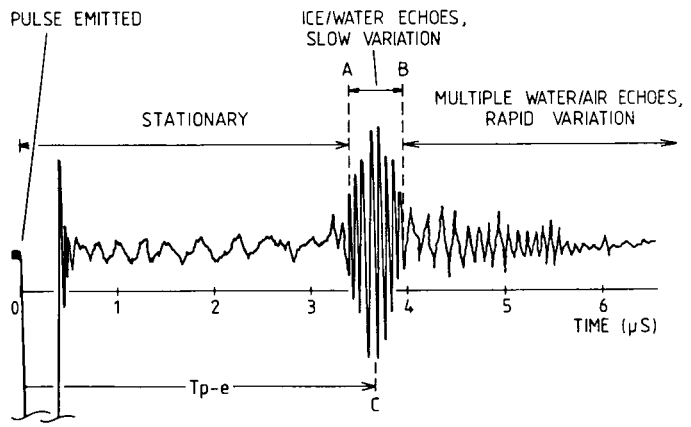

The location of the test cylinder in the tests conducted in the Icing Research Tunnel (IRT) is indicated here.

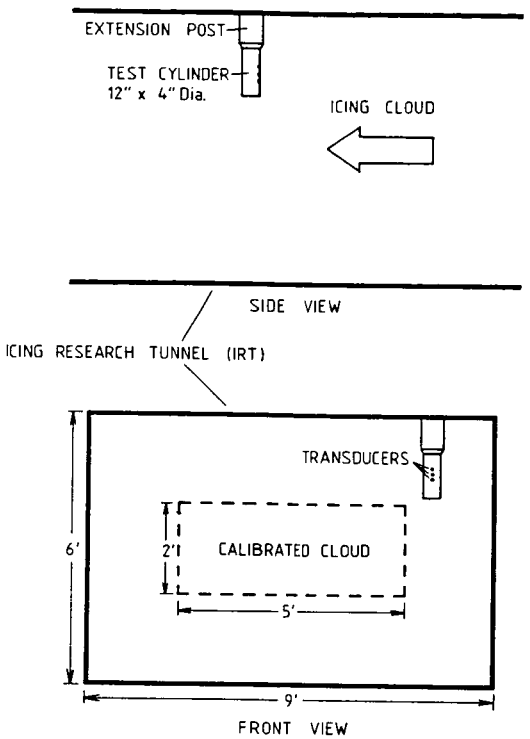

This figure presents ice thickness versus time for light icing conditions measured by ultrasonic transducers on the stagnation line of a 4-in.-diameter cylinder in the IRT.

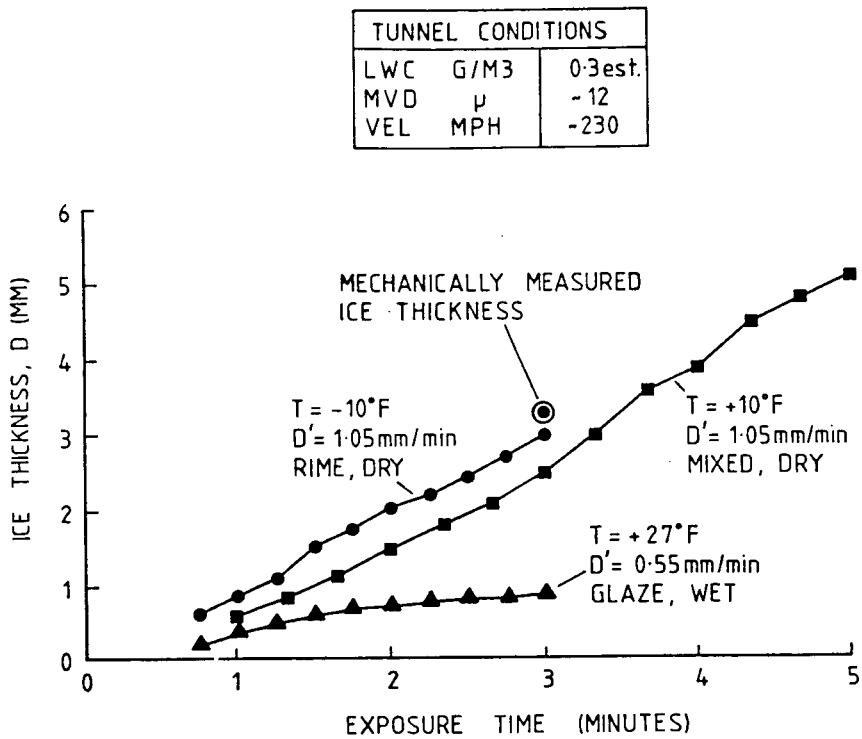

This figure presents ice thickness versus time for heavy icing conditions measured by ultrasonic transducers on the stagnation line of a 4-in.-diameter cylinder in the IRT.

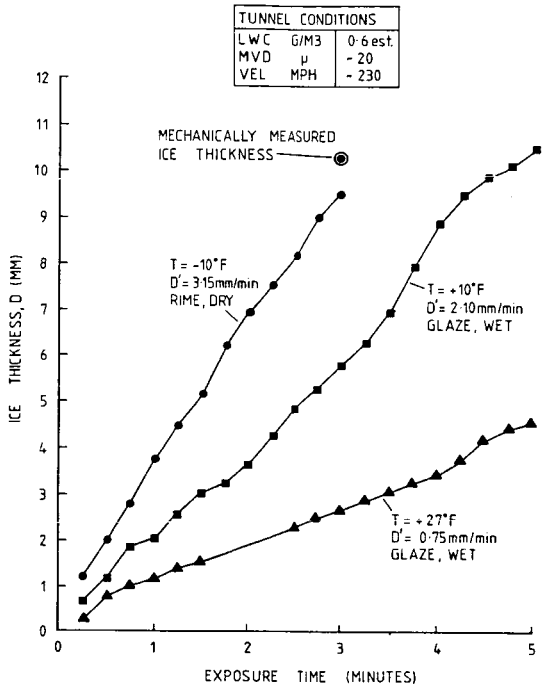

A comparison of ice accretion rates for various tunnel conditions is given in this figure. The accretion rate on the stagnation line is seen to increase with decreasing temperature until dry ice growth is achieved.

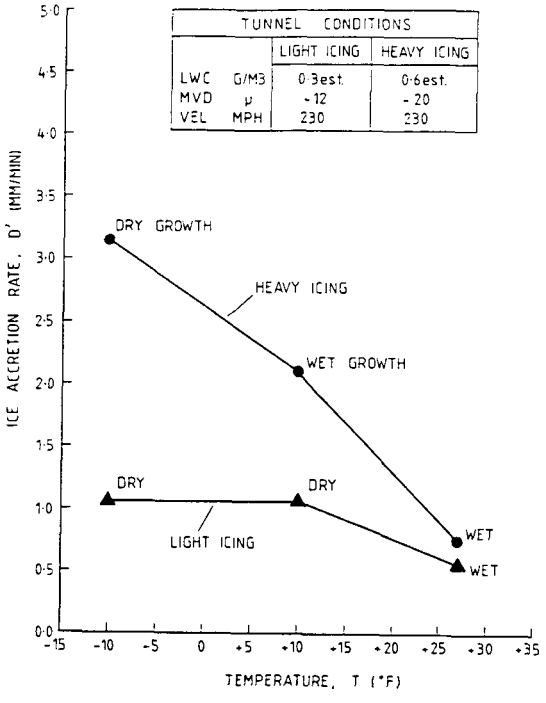

This figure shows the experimental configuration for flight tests of the ultrasonic measurement system mounted on a test cylinder which extended through the roof of the NASA Twin Otter Icing Research Aircraft.

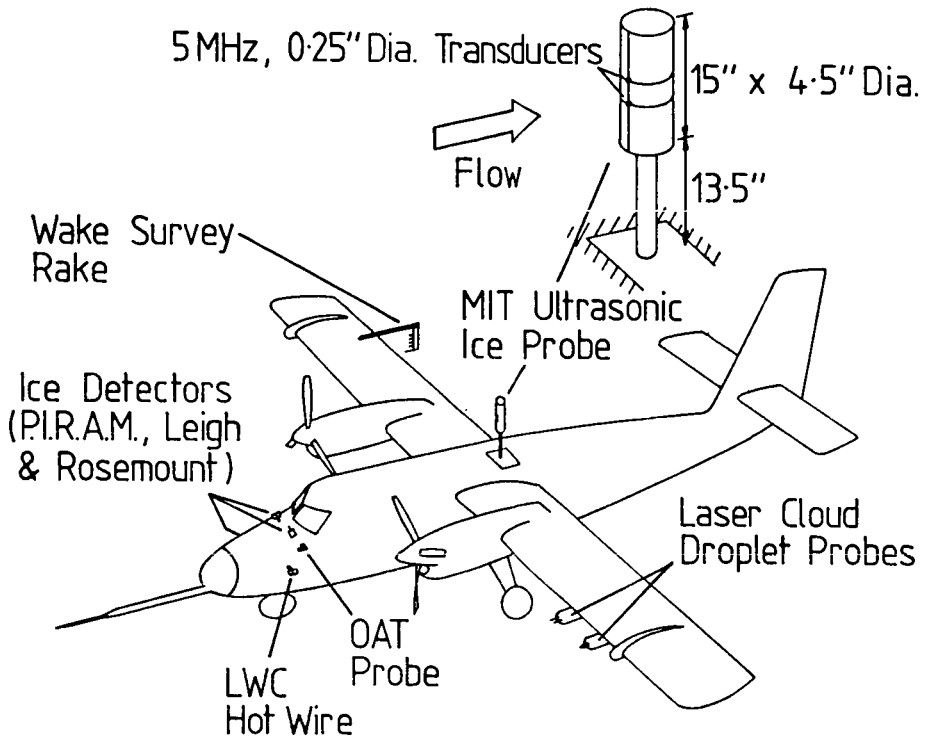

This figure presents a typical plot of ice thickness versus time for natural (flight test) icing conditions. The data shown are from research flight 85-24. Also shown are plots from similar icing conditions in the IRT.

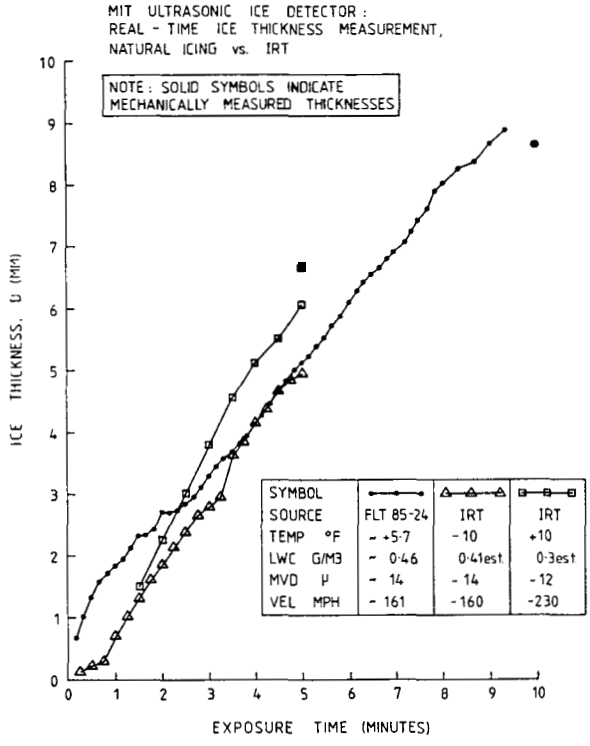

Icing rates versus exposure times (as measured by the MIT ultrasonic, Rosemount and PIRAM detectors on the aircraft for flight 85-24) are shown. Also shown is the cloud liquid water content as measured by the Johnson-Williams probe. For the relatively cold conditions encountered on this flight the icing rate is expected to be directly proportional to the liquid water content.

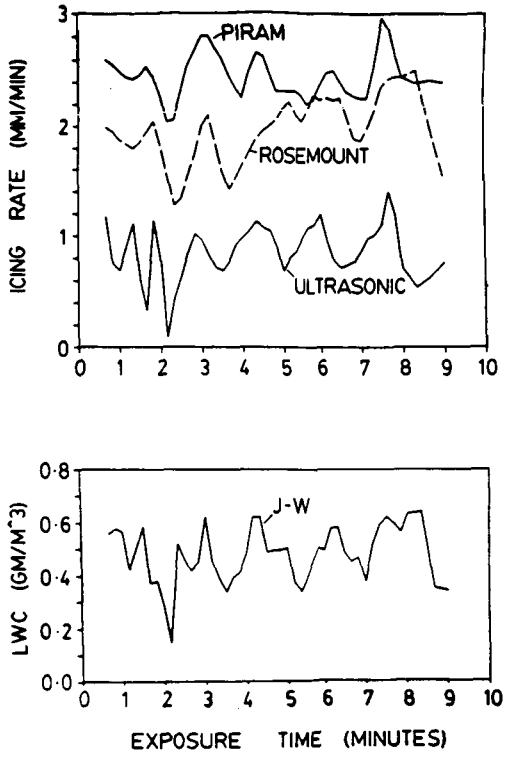

This figure schematically presents the components of the simple heat balance model used to predict wet/dry ice growth. By parametrically comparing the predicted threshold for wet/dry growth with observed wet and dry growths measured by the ultrasonic technique, it is possible to infer data on the heat transfer behavior of the ice surface. This heat transfer behavior is seen as a major area of uncertainty in current ice accretion modeling and scaling efforts.

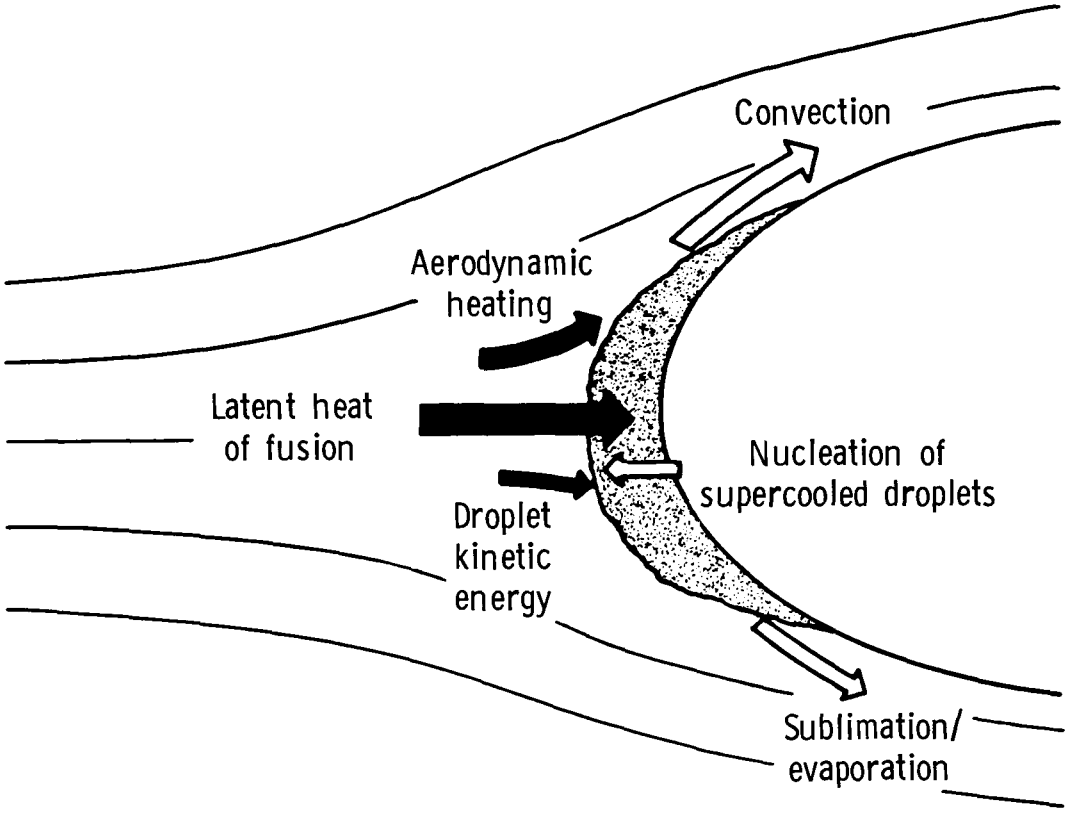

Wet/dry threshold predictions for several heat transfer coefficients along with measured wet/dry from a series of tests in the IRT at 102.8 m/sec are given in this figure. The best agreement to the data is a high heat transfer coefficient characteristic of a high (3.5%) free-stream turbulence level and a rough surface.

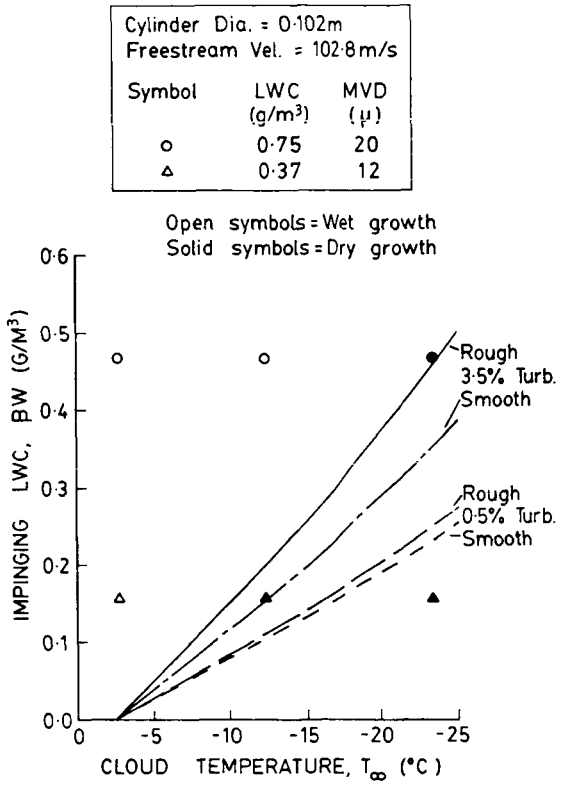

This figure presents wet/dry threshold data for several additional tunnel velocities. The 3.5-percent turbulence model is consistent with the observed data.

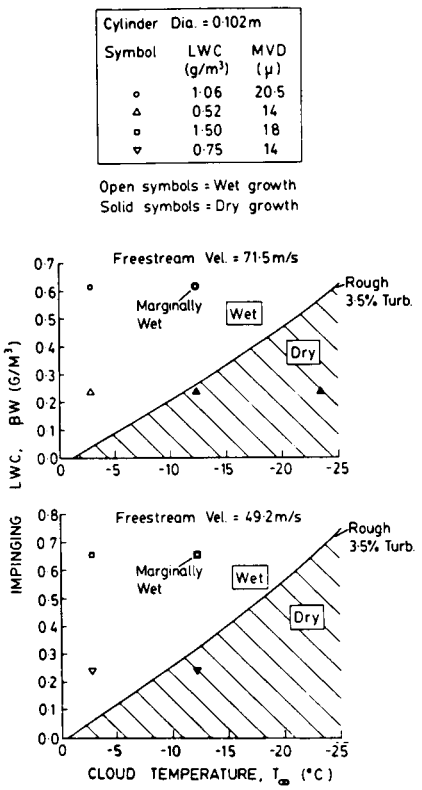

This figure shows the liquid water content versus exposure time for research flight 85-24. Also shown are periods of wet, dry and transitional ice growth. It is important to note that in flight icing conditions the environmental conditions are often unsteady. The fluctuations in liquid water content cause a fluctuating heat load which causes the ice growth to vary from wet to dry in the same flight.

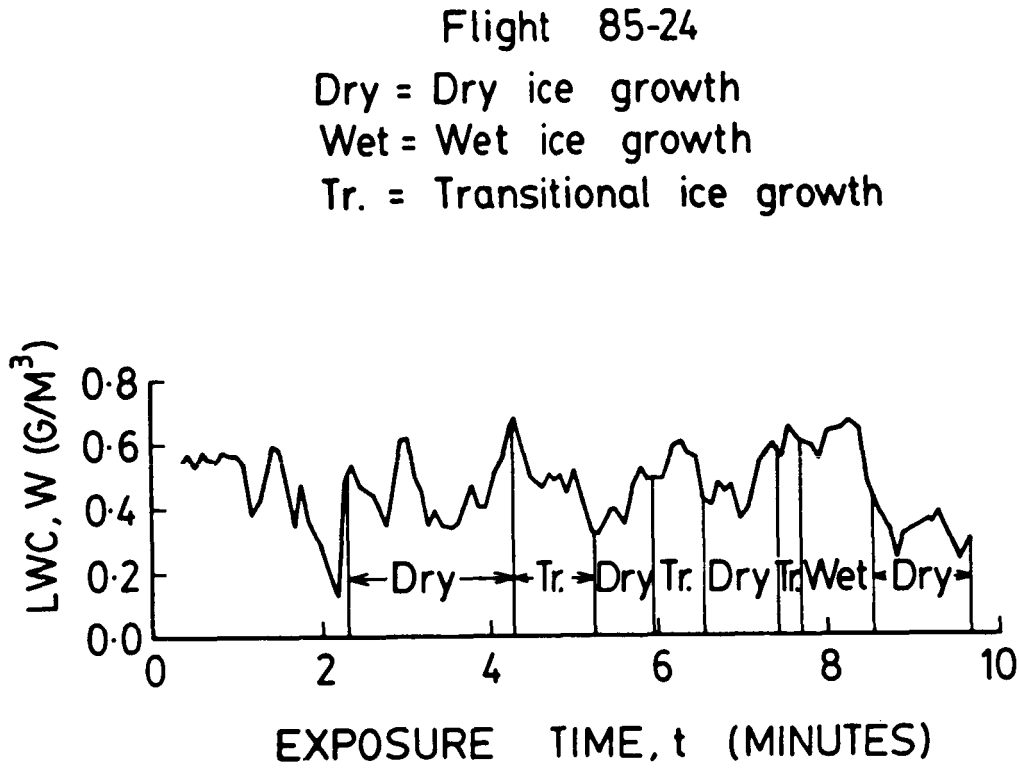

This figure presents wet/dry threshold data for the 1985 flight test series. The heat transfer generally appears to be lower in flight than in the IRT and is consistent with a lower value of ambient turbulence. There is, however, some day to day variation in the heat transfer which is thought to be due to variations in turbulence due to different meteorological conditions. Both the transient nature of the heat load and the effect of variations in the heat transfer due to turbulence level are important to consider when extrapolating wind tunnel results to the flight condition.

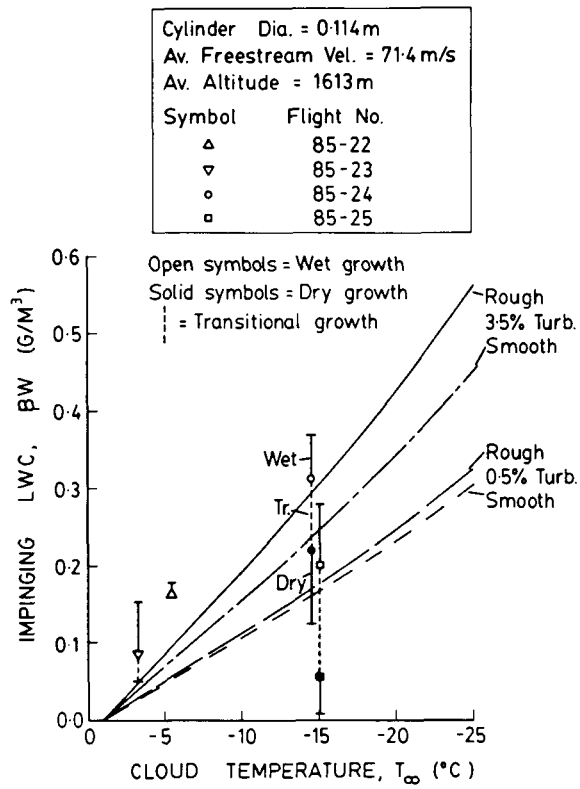

The testing philosophy behind the upcoming flight tests where an array of ultrasonic transducers will be flown on a wing cuff mounted on the right wing of the NASA Twin Otter Icing Research Aircraft is depicted. The cuff will be tested both in natural (flight) conditions and in the IRT under similar icing conditions. In addition, the same 2-D airfoil will be subject to analysis by analytical models and scaling criteria. This data set will provide a unique opportunity for the direct comparison of the various icing analysis and certification tools currently being used.

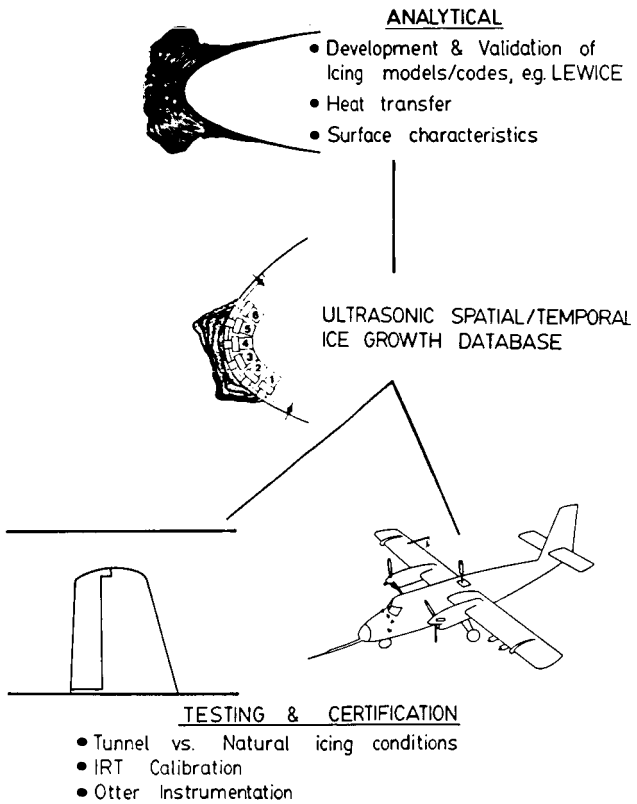

This figure shows the location of the wing cuff on the NASA Icing Research Aircraft.

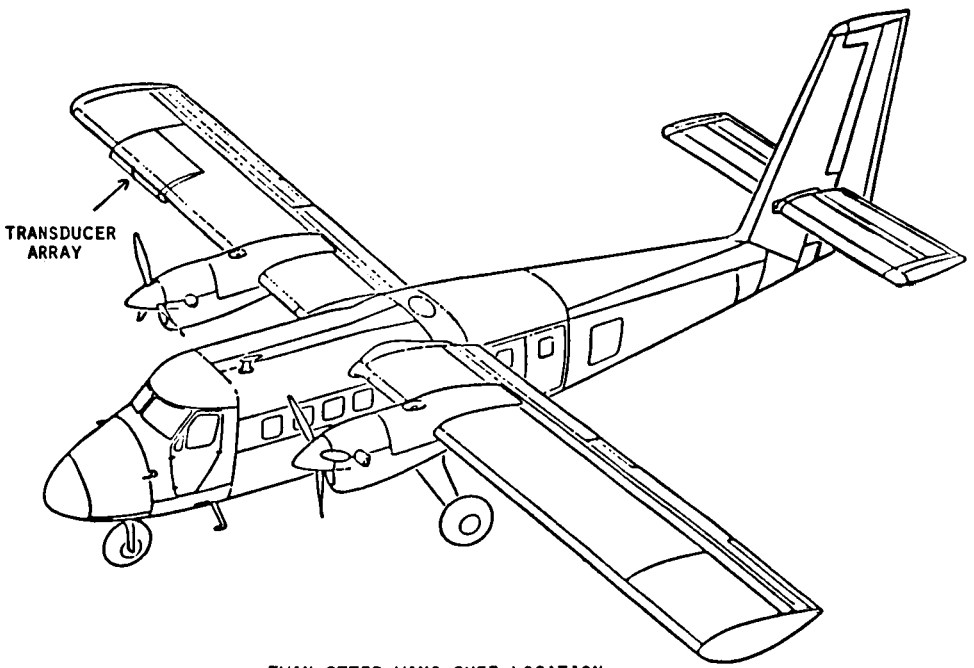

TWIN OTTER WING CUFF LOCATION

A schematic view of the data acquisition system to be used in the array flight tests is shown in this figure.

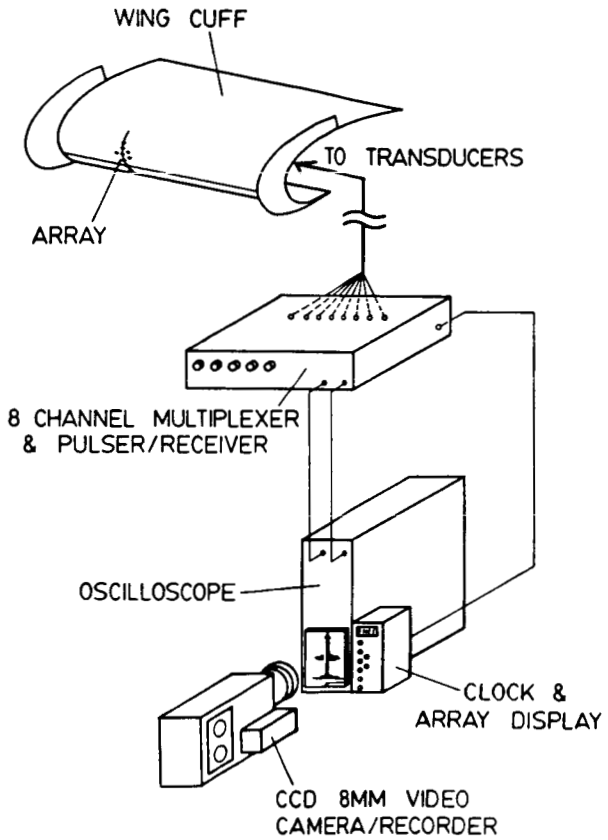

FAA/NASA JOINT UNIVERSITY PROGRAM

IN AIR TRANSPORTATION SYSTEMS

R. W. Lilley
Ohio University
Athens, Ohio

INTRODUCTION

Four areas of activity received emphasis during the year. Three of these areas continued into 1986, with the addition of a Multisensor Navigation study.

The Loran-C navigation system has kindled intense interest among the aviation user community, and this interest has been made known to FAA. Current efforts to define non-precision approach procedures based on Loran-C are involving many FAA segments in a cooperative program with the users. Loran-C accuracy is not questioned; assurance of signal integrity and the criteria for receivers and flight-check measurements are still under study.

Ohio University is operating Loran-C monitors at Athens and Galion, Ohio, measuring signal stability as a function of weather and time of day in support of the general push toward IFR approach use of the system.

The Global Positioning System will offer positioning and navigation services available to the aviation community in the 1990s and beyond. The same signal integrity and monitoring issues must be handled as for Loran-C. ATC integration will be similar to Loran-C. In short, we are practicing for global system positioning (GPS) as we prepare for enhanced Loran use in the instrument flight rules (IFR) airspace. GPS receiver designs for low-cost production are being considered.

The DATAC digital avionics bus monitor test bed unit is nearing completion, and the final report is expected during the coming year. This unit will permit development or test personnel to exercise the data bus and its associated terminals and to perform data loop-back testing by writing user test programs based on software primitives provided with the unit.

The fiber-optic data bus was successfully demonstrated, and this portion of the program halted for the present to permit added emphasis in the other areas of study.

The expectation is that multiple-sensor (for example GPS/inertial) navigation systems will become desirable in the near future and that such systems will offer services which may be in demand for at least the upper general-aviation market. To understand the sensors, blending algorithms and appropriate display devices, a literature search and planning have been initiated.

ANNOTATED BIBLIOGRAPHY*

No. 94 "GPS Antenna Survey"
Samuel J. P. Laube, March, 1985, 33 pages.

Success of the Global Positioning System (GPS) navigation scheme for civilian aviation use requires a durable, inexpensive, light-weight antenna. A survey of available commercial antennas and construction information is given to allow easy implementation of the most economical design choice.

No. 95 "LORAN-C Monitor Technical Manual"
Jamie Edwards, May, 1985, 131 pages.

The design and implementation of the LORAN-C Monitor, stationed at Galion, Ohio, are explained. The data collected can be used to analyze LORAN-C signal variations over daily and seasonal cycles for use in non-precision approach studies.

No. 96 "Fiber Optic Data Bus"
Michael A. W. Lenz, June, 1985, 19 pages.

The construction and operation of an optical fiber data bus are described with an application to aircraft instrumentation.

No. 97 "Operational Considerations for LORAN-C in the Non-Precision Approach Phase of Flight"
Robert W. Lilley, Daryl L. McCall, August, 1985, 14 pages.

Ground monitor data collected at Galion and Athens, Ohio, are presented, with assessment of correlation over the 90 nm between the two sites. Flight data collected on runways 7 and 25 at Ohio University airport are discussed in terms on non-precision approach requirements; effects of waypoint resolution and receiver cycle-slip are noted. Comments are included on data collection methods.

No. 98 "Investigation through Simulation Techniques of the Application of Differential GPS to Civil Aviation"
Daryl L. McCall, August, 1985, 104 pages.

This paper investigates the potential of differential GPS to provide a Category I precision approach to landing for civil aviators. Within the text is a discussion of conventional and differential GPS characteristics and techniques. Emphasis is given to the simulation models used to produce the results presented in the paper.

*Ohio University entitles these reports Ohio University NASA reports; they should not be confused with NASA's technical reports.

Nos. 99 through 103 "FAA/Ohio University LORAN-C Monitor; Athens, Ohio" Jamie Edwards, November, 1985, 147 pages total.

These reports contain raw data, which are subject to further processing. They are provided for the purpose of supplying timely preliminary information.

GPS EXPERIMENTS

N87-27599

Samuel J. P. Laube
Ohio University
Athens, Ohio

OVERVIEW:

Current funding of the FAA/TRI-U has been used for experimentation and exploration of the Global Positioning System (GPS). A method of collecting positional data has been devised using the FAA receiver built by Lincoln Labs which was originally designed for service as a long-term fixed monitoring station. Modification of the receiver continues and this will allow usage as an aircraft navigator.

Additional effort has been spent on development of an experimental receiver or test bed receiver that would allow modification and implementation of new GPS receiver design concepts. This receiver design is still in the concept stage, but is near completion and will stress low cost and application to the civilian aviation community. The receiver design will provide an ability to make design decisions and perform implementation in experiment form for proof of design.

The Lincoln Labs receiver will allow immediate ability to collect positional data while in flight. This ability allows a unique opportunity that will be immediately available to the center. Development of the test bed receiver will also allow for more flexible experimentation not currently available with the Lincoln Lab receiver.

PROBLEMS:

Problems with the Lincoln Lab receiver are being solved. This particular system requires excessive power and weight requirements not available in single engine aircraft. The Center has available a DC-3 aircraft that will more than meet the requirements of the Lincoln Lab receiver cargo. Some minor modifications and engineering tasks are being solved so the Lincoln Lab receiver can be installed in the DC-3 with minor modifications. Current status of the installation is being performed by this engineer with assistance of the aircraft's flight mechanic. Construction of the power wiring harness is complete, as are installation of the power inverters. Rack mounts are installed in the DC-3, and construction of the signal and control wiring harness is in progress. Several initial problems with the Lincoln Lab receiver have delayed installation, stemming from failed circuit traces on a three-layer processor board. These traces have been located and are being repaired with available tools. Assistance from Chuck Harris of STI has been invaluable with repair.

Most of the problems are related to the STI receiver component in the Lincoln Lab receiver, which was constructed as a prototype several years ago, and is starting to show age.

The goal of the test bed receiver design is to make it inexpensive and flexible. The current effort is directed toward developing a minimum cost Doppler tracking mechanism. This presents a problem because of the unique spread spectrum nature of the GPS code. A low-cost alternative to coded cross correlation is being investigated.

RESULTS:

Data collection for fixed position at two locations has been accomplished using the Lincoln Labs receiver. This enables troubleshooting and also data collection. A constant error in positional location regardless of location or time has been noted. This bias is probably due to an algorithmic problem in the receiver design. Modification of the receiver algorithm must take place. This will require expansion of the receiver management computer's memory capabilities. Plots of positional error from a known benchmark are shown. These are for three-dimensional error of Earth-centered position fix, as well as the individual components. The plots show six satellites, five satellites and finally a minimum of four satellites. As expected, the positional error with four satellites suffers from noise degradation due to geometric dilution of position (GDOP).

Receiver concepts are currently being proven with theoretical methods for performance comparison, as well as function. A final design proof is nearing completion. Implementation of this proof into hardware will provide the basis of a Doppler tracking device. Future pathways and possible developments will also arise with this component completion. Explanation of the basic code tracking concept is included in one of the following figures. Improvements for this design approach are currently being developed. The end result will be a flexible approach to codeless Doppler tracking. This will provide the core function of the test bed receiver. Added functions that can be developed will be intelligent loop control and tracking abilities, as well as implementation of navigation algorithms and conservation of loop resources.

CURRENT PROJECTS :

FAA RECEIVER FLIGHT

GPS DOPPLER TRACKING LOOPS

FAA RECEIVER FLIGHT

CONTINUED TROUBLE WITH THE STI RECEIVER .

- TRACKED TO AN INTERMITTENT TRACE ON THE CHANNEL 2 PROCESSOR CARD.
- TRACE NOT LOCATED YET DUE TO MULTILAYER.
- OBTAINED INFO AND PARTS FROM STI.

DC-3 POWER PANEL COMPLETE

- TESTED DUAL INVERTERS WITH NO LOAD.
- INSTALLED 28/120 VOLT WIRING OUTLETS AND PROTECTORS.
- INSTALLED METERING.

FAA RECEIVER FLIGHT

GROUND TESTS :

- OPERATED STI RECEIVER AT ALBANY LABS.
- COLLECTED FIXED POSITION DATA.

KNOWN BENCHMARK :

LATITUDE 39° 12' 39.803"

LONGITUDE -82° 13' 29.709"

ALTITUDE 196.06 Meters

GPS POS, ERROR

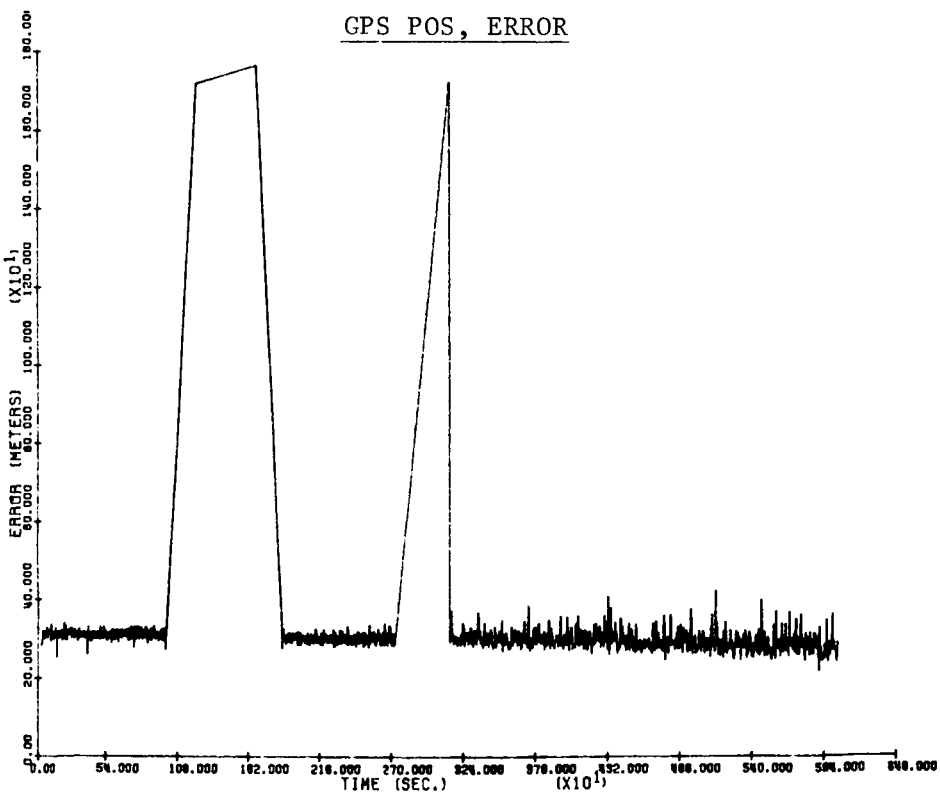

GPS RMS X-Y-Z ERROR

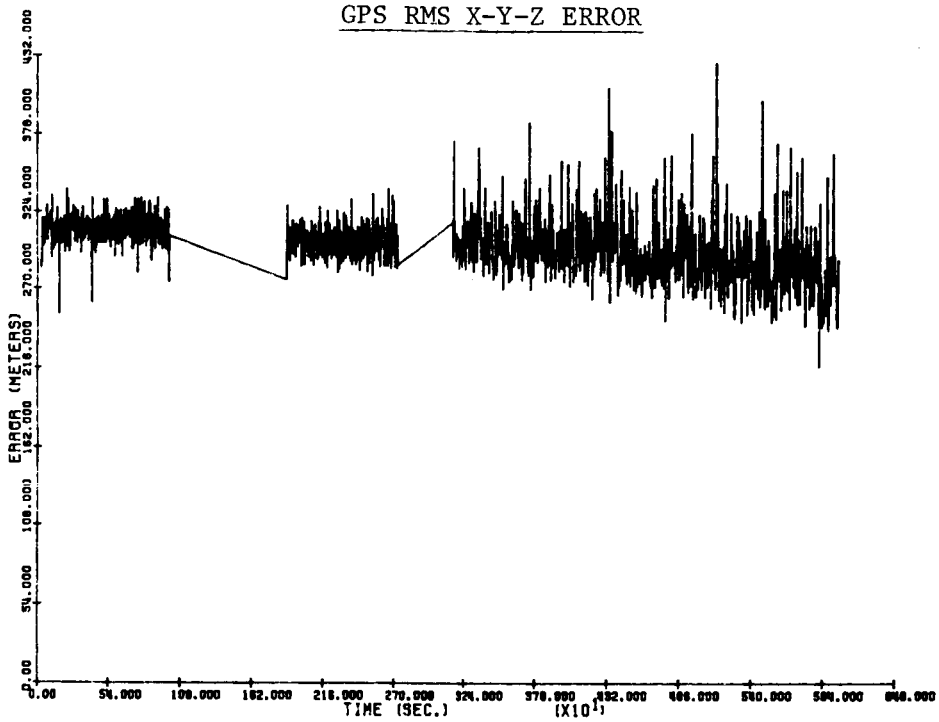

GPS X POS. ERROR

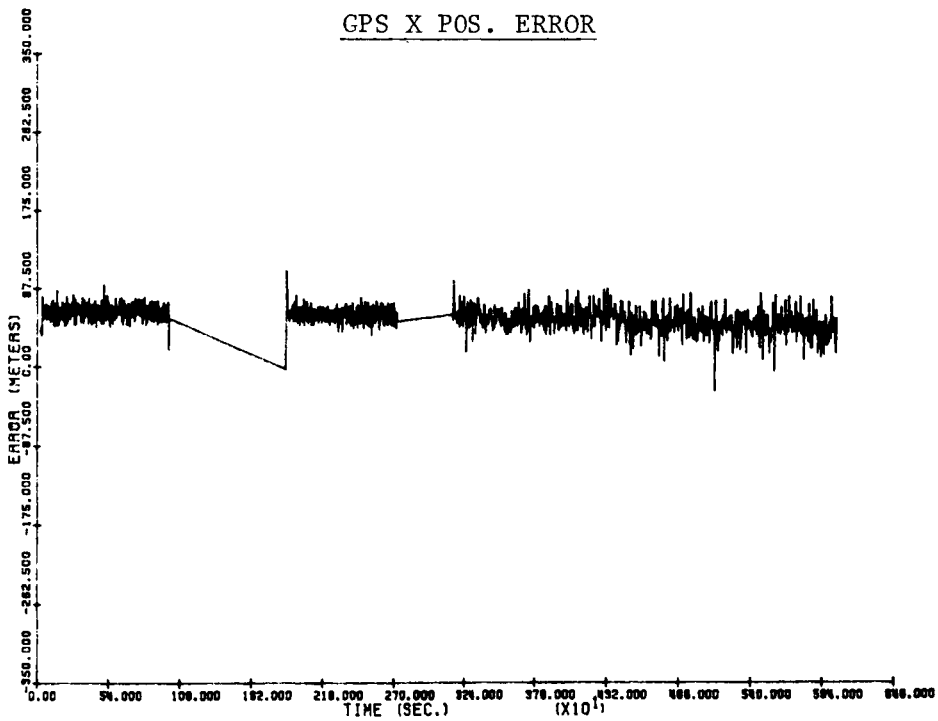

GPS Y POS. ERROR

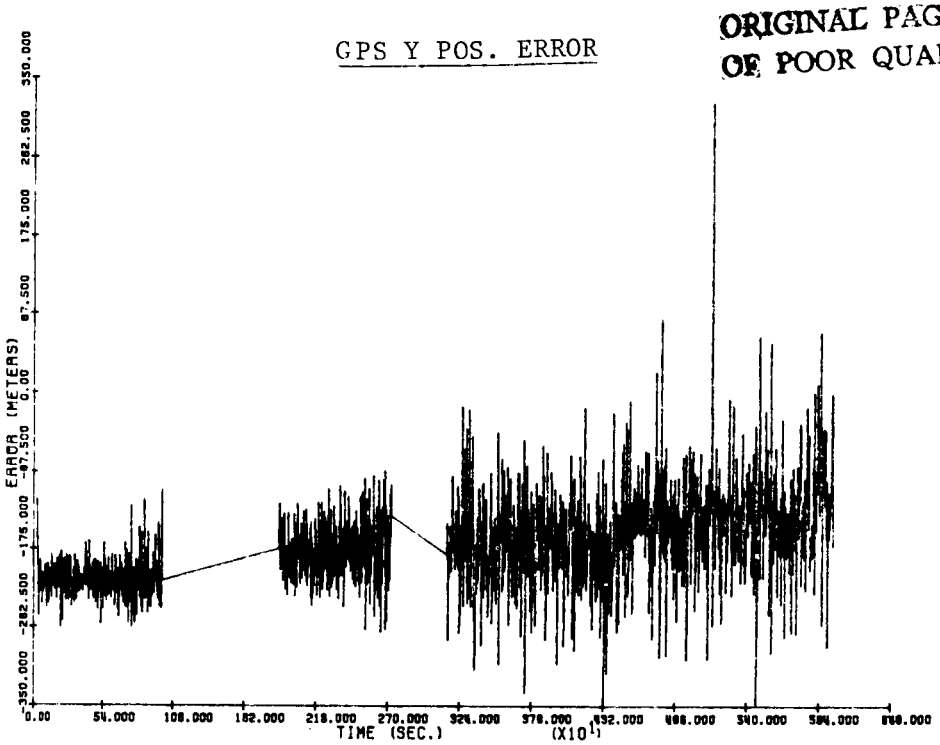

GPS Z POS. ERROR

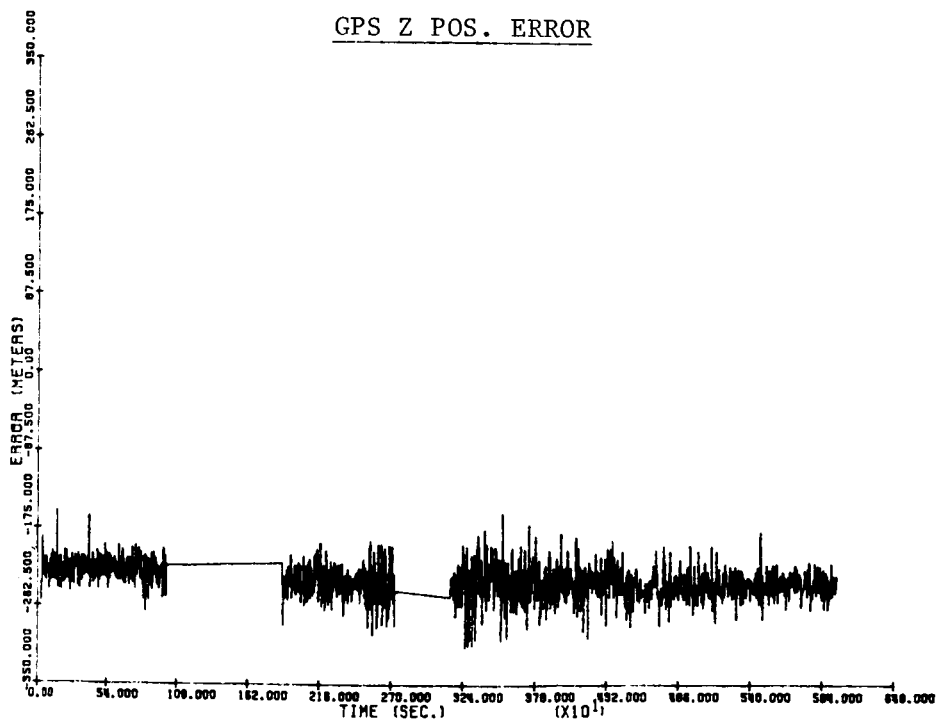

GPS DOPPLER TRACKING LOOPS

- ANALYSIS OF AUTOCORRELATION CONTINUES FOR SIMPLIFIED CASE.

- ANALYSIS OF DELAY LOCK LOOP CONTINUES FOR SIMPLIFIED CASE.

- COMPUTER SIMULATIONS OF ACTUAL C/A $\otimes$ D CODES.

ANALYSIS OF DELAY LOCK LOOP FOR 3-BIT CODE SEQUENCE

EXPRESSION FOUND :

$$X(t) = \sum_{N=2}^{\infty} \delta(t - N\tau)$$

FOR

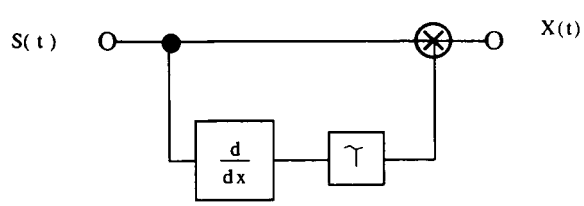

INTEGRATING X(t) YIELDS CODE CLOCK REPLICA.

LORAN-C MONITORING

N87-27600

Jamie Edwards
Ohio University
Athens, Ohio

The Loran-C monitor developed by Ohio University will collect Loran signal data for storage on magnetic tape. Stationed at the Ohio University Airport, Athens, Ohio, the monitor will provide valuable information concerning the daily and seasonal variation of the Loran-C signals for use in non-precision approach studies. With the aid of a second monitor, located in Galion, Ohio, it can be determined if the errors found at a particular geographic location correlate with those found at another location. This will provide some indication as to how far apart future monitors can be positioned to obtain accurate non-precision approach data for various airports.

The monitor uses an ARNAV AVA-1000 Loran-C receiver, which provides outputs of TD's, SNR's, signal strengths, and envelope-to-cycle discrepancies once per 60 seconds. The monitor computer, a Commodore 64, averages five such outputs and assigns a time stamp which is the time-of occurrence of the third sample.

A uninterruptable power supply (see figure 1) was added to keep the monitor operating during short-period power outages. Along with this, a heating system was provided to keep the monitor operating during the cold winter months.

Work this year has been devoted to data collection, data reduction, plot generation, and general monitor maintenance (fig. 2).

Five technical memoranda have also been written containing plots of TD's and SNR's from June through October's Loran-C data. These reports represent the first few in a series containing interim raw data collected from the Loran-C monitor located at the Ohio University Airport, Athens, Ohio. Listed below are the reports already written:

TM (NASA) 99 FAA/OHIO UNIVERSITY LORAN-C MONITOR
INTERIM DATA REPORT NO. 1

TM (NASA) 100 FAA/OHIO UNIVERSITY LORAN-C MONITOR
INTERIM DATA REPORT NO. 2

TM (NASA) 101 FAA/OHIO UNIVERSITY LORAN-C MONITOR
INTERIM DATA REPORT NO. 3

TM (NASA) 102 FAA/OHIO UNIVERSITY LORAN-C MONITOR
INTERIM DATA REPORT NO. 4

TM (NASA) 103 FAA/OHIO UNIVERSITY LORAN-C MONITOR
INTERIM DATA REPORT NO. 5

A literature search, already under way, will contain collected information from various dial-up data base information services. This information will be used to write a report on Loran-C navigation systems (fig. 3).

CIRCUIT DESIGN OF BACKUP SYSTEM

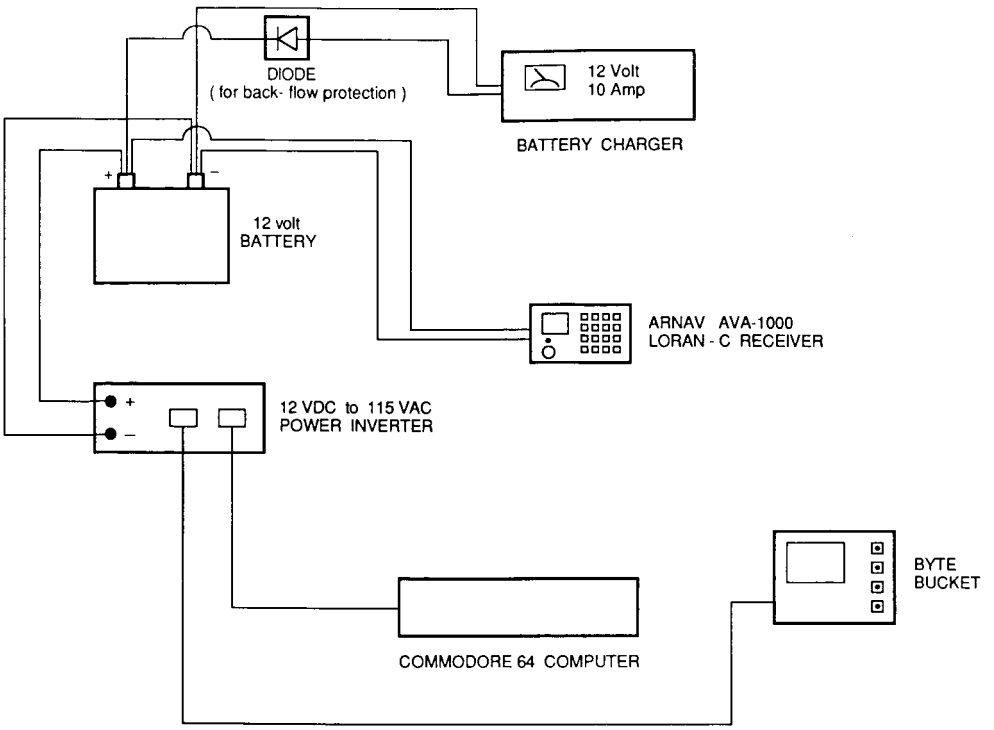

Figure 1

TASKS COMPLETED THIS PAST QUARTER

* MAINTAINED MONITOR
* TRANSFERRED DATA COLLECTED ON BYTE BUCKET CASSETTE TAPES TO MAGNETIC TAPES
* PLOTTED LORAN - C TD'S AND SNR'S FOR TECHNICAL MEMORANDA
* INSTALLED A HEATER IN THE BUILDING WHERE THE MONITOR IS LOCATED
* INSTALLED BACK-UP POWER SYSTEM FOR THE MONITOR
* STARTED LITERATURE SEARCH

Figure 2

FUTURE PLANS

* CONTINUE TO MAINTAIN MONITOR
* REDUCE AND PLOT DATA FOR TECHNICAL MEMORANDA
* CONTINUE LITERATURE SEARCH AND WRITE REPORT ON LORAN-C NAVIGATION SYSTEMS

Figure 3

DIGITAL AUTONOMOUS TERMINAL ACCESS COMMUNICATIONS

S. Novacki
Ohio University
Athens, Ohio

DATAC BUS MONITOR

A significant problem for the Bus Monitor Unit is to identify the source of a given transmission. This problem arises from the fact that the label which identifies the source of the transmission as it is put onto the bus is intercepted by the DATAC terminal and removed from the transmission. Thus, a given subsystem will see only data associated with a label and never the identifying label itself. For normal bus subsystems, this presents no problem as each subsystem anticipates using only certain pieces of information and is capable of dealing with those pieces of information within the time frame between datum updates. The Bus Monitor, however, must not only receive all information that is present on the bus, but identify the source of the transmission so as to be able to provide some type of error identification/location in the event a problem with the data transmission occurs.

To alleviate this problem, we take advantage of a design feature of the DATAC terminal. The terminals can be programmed to produce an interrupt vector and an interrupt strobe upon receipt of a label. Ordinarily, this would be used to alert the subsystem connected to that bus terminal that a certain block of data has been received and to begin processing it. Again, because of the general nature of the Bus Monitor Unit, we need to process all the information that appears on the bus. When a second block of data arrives, we may not be done processing the first block, but we still want to know that the second block has arrived. Our solution is to allow the DATAC terminal to produce the interrupt signal, along with some arbitrary interrupt vector that we shall simply consider to be an identifying tag, rather than the address of a service routine. As a transmission is received, the transmission label is recognized by the terminal, produces the interrupt strobe and at the same time places the appropriate interrupt vector/tag on the address lines. The vector/tag is captured in a 16-bit register which is mapped into the I/O space of the Bus Monitor's Z8000 CPU. The Z8000 can then interrogate this register as needed to determine the source of the latest transmission. The interrupt strobe is directed to a transmission gate controlled by the Z8000 whose output is in turn connected to the gate controlled by the Z8000 whose output is in turn connected to the NMI/VIx lines the CPU. Additionally, the DMAREQ* signal from the Subsystem Interface of the DATAC terminal is now ORed with a control signal from the Z8000 that allows the Bus Monitor to inhibit a DMA operation. This permits the Bus Monitor to complete any pending processing tasks before being interrupted by a new block of data. By gating off the NMI/VIx associated with the new transmission, we now have the option of being immediately alerted to the arrival of new data or *DMA Request.

ignoring a given transmission until we have completed processing the last data received. This feature would prove useful when monitoring the communication schedule of the DATAC bus. In this mode, we are not concerned so much with the data that appears on the bus, but rather simply that each unit is communicating in the proper time frame.

With these modifications, the Bus Monitor processor may now identify the source of the data it receives, as well as control its reception of that data. These capabilities become increasingly important as the Bus Monitor is required to perform more and more complex data reduction tasks.

DATAC Terminal Interrup Monitor

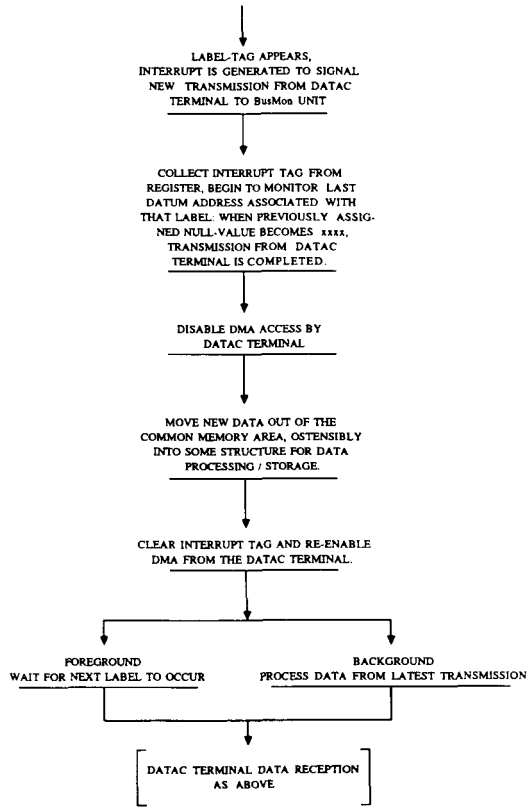

Bus Monitor Memory Map

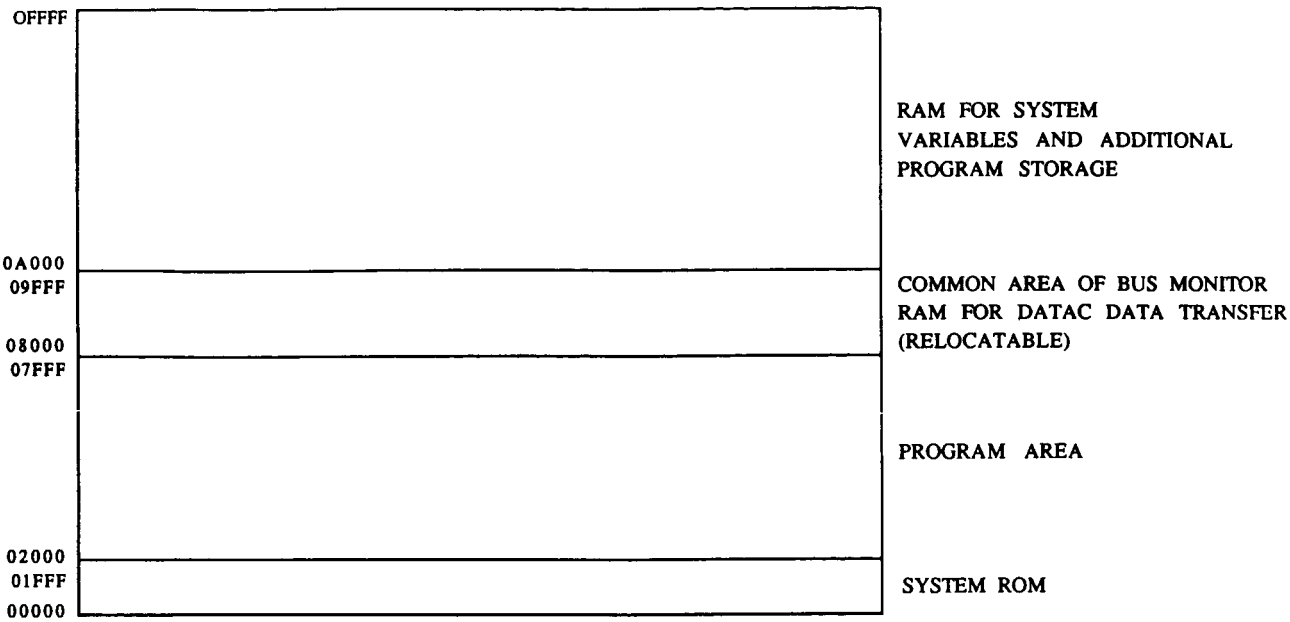

Data Terminal Transmission Identification and Acquisition

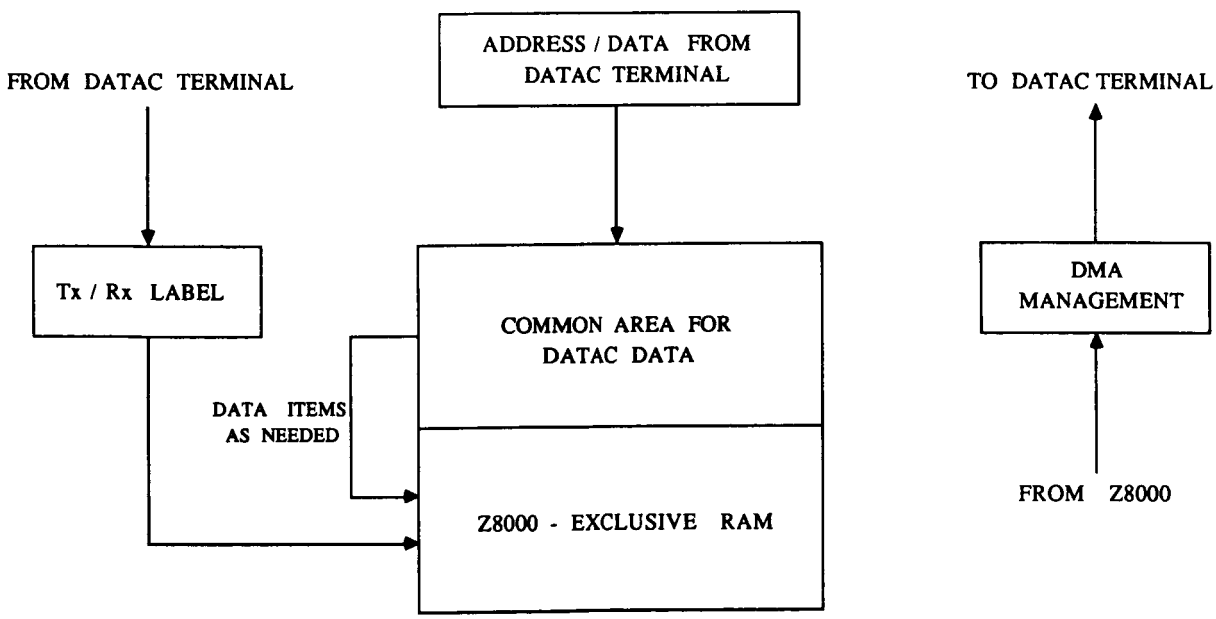

Modification to ZBUS/IEE696 Interface
To Allow Tranmission Identification

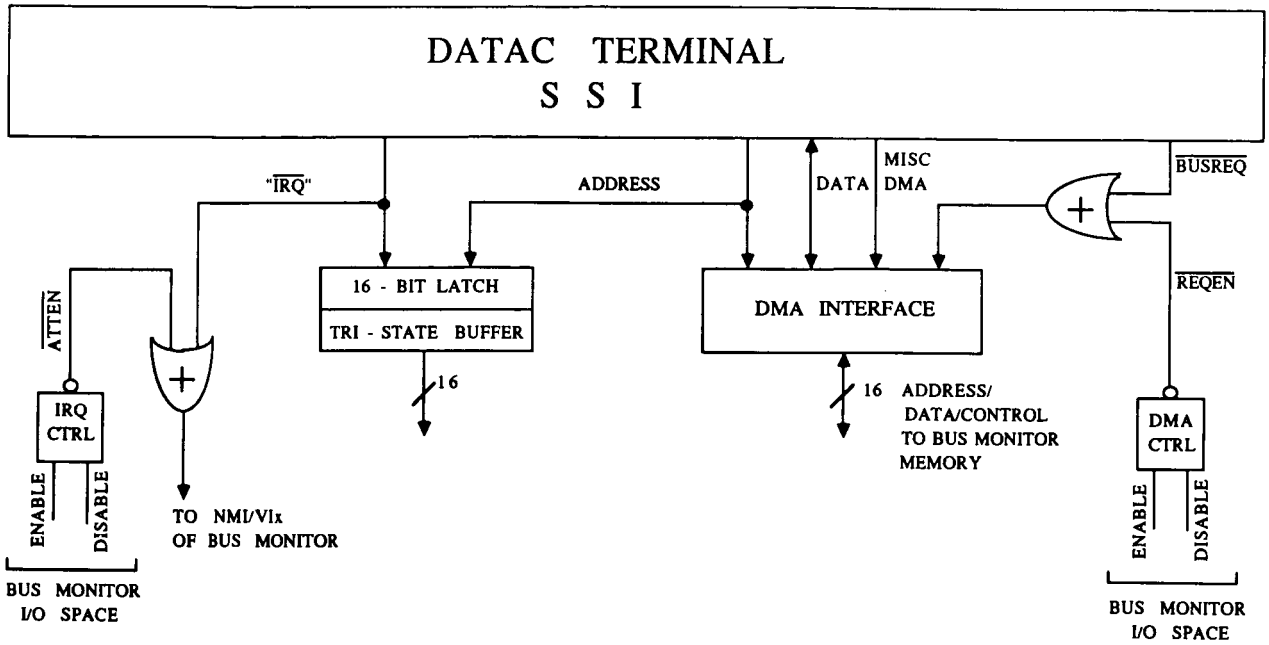

N87-27602

INERTIAL/MULTISENSOR NAVIGATION

Dimitri Alikiotis
Ohio University
Athens, Ohio

The purpose of any Navigation System is to determine a vehicle's position while the vehicle is moving or it is stationary. There are many different kinds of Navigation Systems, each one based on a different principle. These principles include Radio Navigation (LORAN-C), Satellite Navigation (GPS), Inertial Navigation (INS), Low-Frequency Radio Navigation (OMEGA), etc. For Terminal Area Guidance systems such as the Microwave Landing System (MLS) or the Instrument Landing System (ILS) a combination of principles is used. Each navigation system provides different navigational accuracies. For example, the Global Positioning System provides high accuracies for long-term navigation but low accuracies for short-term navigation. On the other hand Inertial Navigation provides high accuracies for short-term navigation but low accuracies for long-term navigation. The Multi-sensor Navigation System incorporates several different Navigation Systems in one. In this configuration the combination of several systems can provide higher navigational accuracies and better system reliability.

The Inertial Navigation System makes use of the vehicle's accelerations in all directions. By integrating these accelerations once, the vehicle's velocity is determined, by integrating twice, the vehicle's position is determined (see Fig. 1). The Inertial Navigation System establishes a three axes reference frame and measures the vehicle's accelerations along these axes. Then a double integration determines the vehicle's relative position and a relative position vector is established. Finally, the Inertial Navigation System has to determine the vehicle's position with respect to Earth. For this purpose the inertial axes have to be constantly aligned with the Earth's pre-established axes. Therefore since the Earth rotates, the Inertial axes have to rotate too. Figs. 1-2 show a simplified Inertial Platform on which three accelerometers are sensing accelerations in three dimensions. The Inertial Platform is supported by the gimbals which serve the purpose of maintaining the precise orientation of the Platform. The Platform gimbals receive information from the System's Gyroscopes and the System's Computer and make sure that the Platform is always level to the Earth's surface and aligned towards a specified direction. Fig. 3 shows the block diagram of a system mechanized in spherical coordinates, in which longitude (ϕ), latitude (λ) and height (R) are supplied. It should be noted that gravity introduces unwanted components in the measured accelerations and these have to be accounted for and cancelled by the System otherwise positional errors will occur and the navigational accuracy will degrade significantly. Another form of the Inertial Navigation System is the Strap-Down system (see Fig. 4), in which the accelerometers are mounted on the vehicle's frame. In this configuration the Navigation Computer plays the role of the gimbals, therefore all the unwanted gravity components are computed and canceled by the Computer. The Computer is also responsible for rotating the pre-established reference frame according to the Earth's rotation.

Fig. 5 shows a Multisensor Navigation System as proposed by the Ohio University Avionics Engineering Center. The proposed system incorporates Radio (LORAN-C), Satellite (GPS) and Inertial (INS) Navigation. The Inertial part of the system will be of low grade since the INS will be used primarily for filtering the GPS data and for short term stability. LORAN-C and GPS will be used for long term stability. Fig. 6 shows different Navigation Systems and their characteristics.

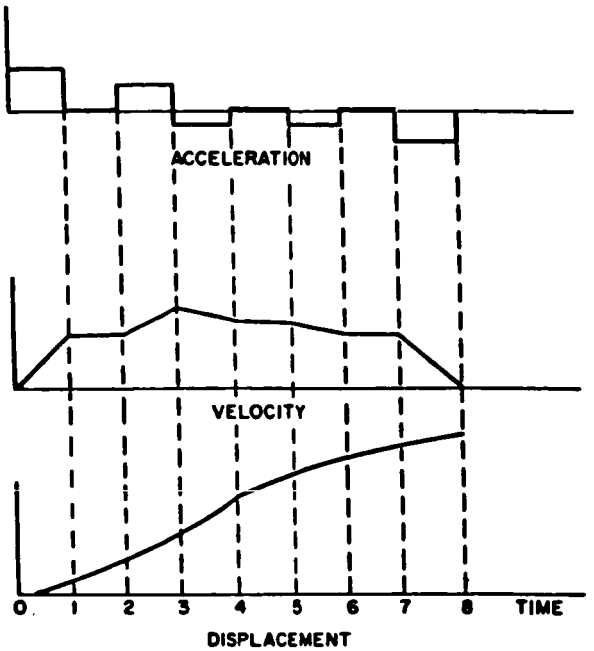

Figure 1. Integration of acceleration.

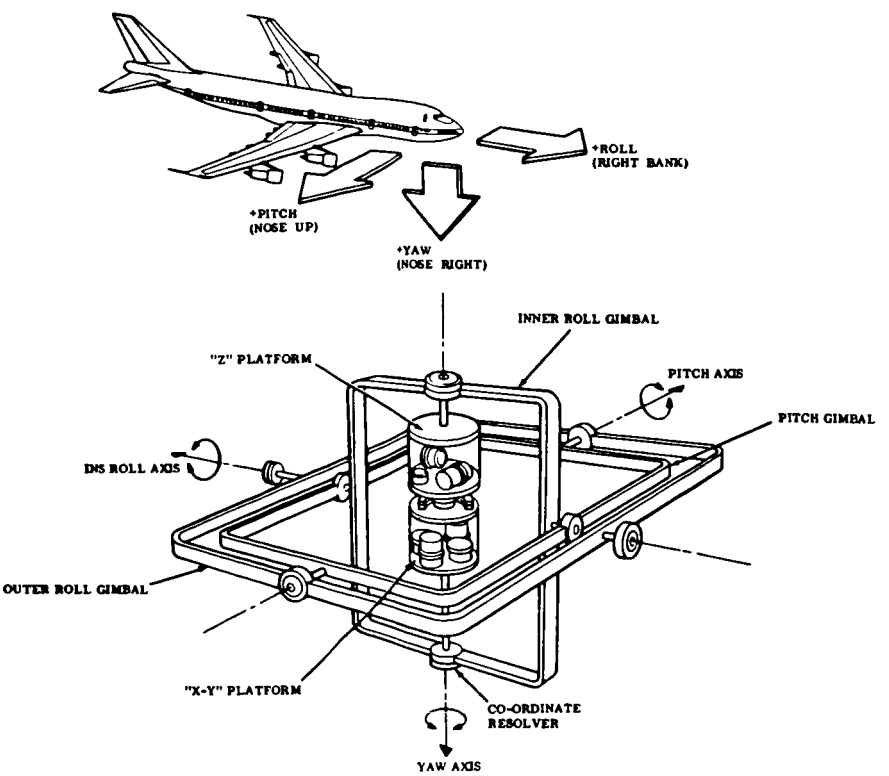

Figure 2. Carousel IV model platform.

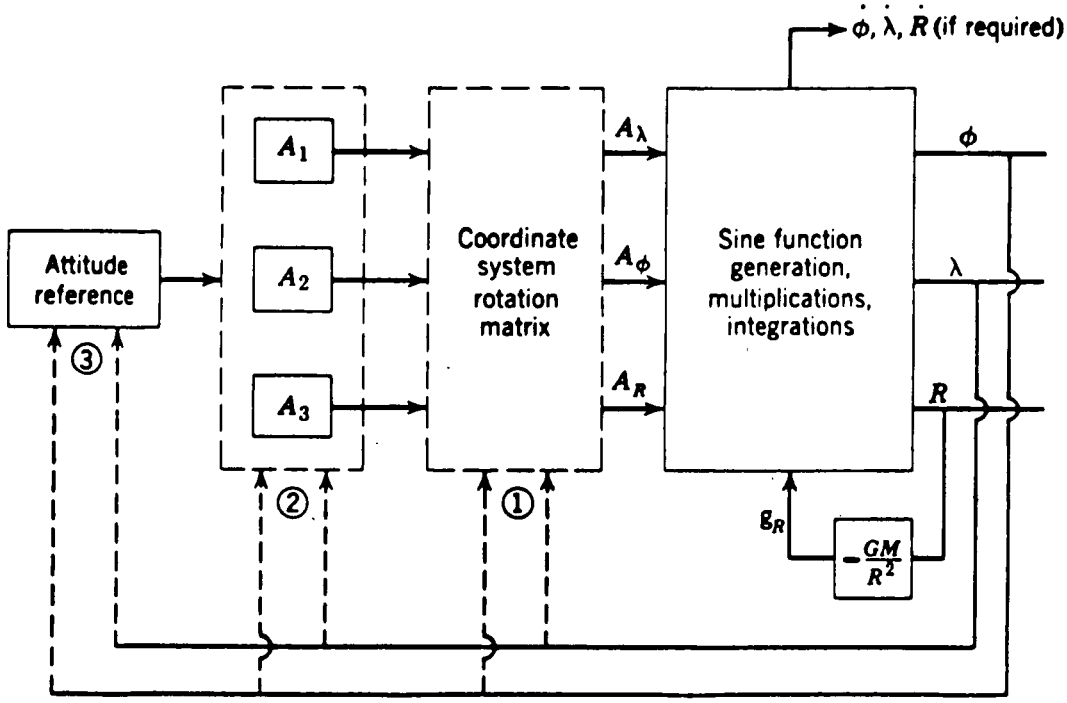

Figure 3. Functional block diagram of an inertial navigation system mechanized in spherical coordinates.

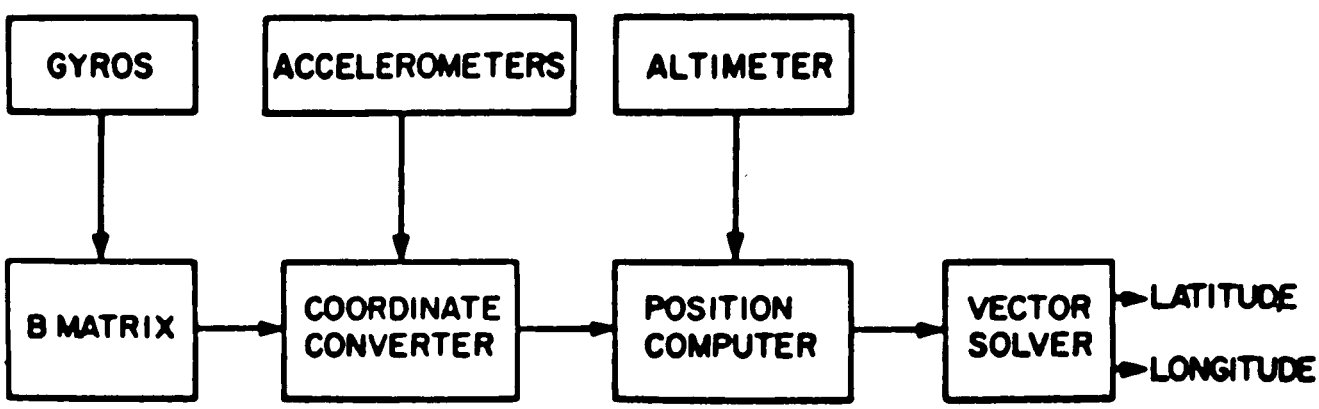

Figure 4. Simplified strap-down inertial navigation system.

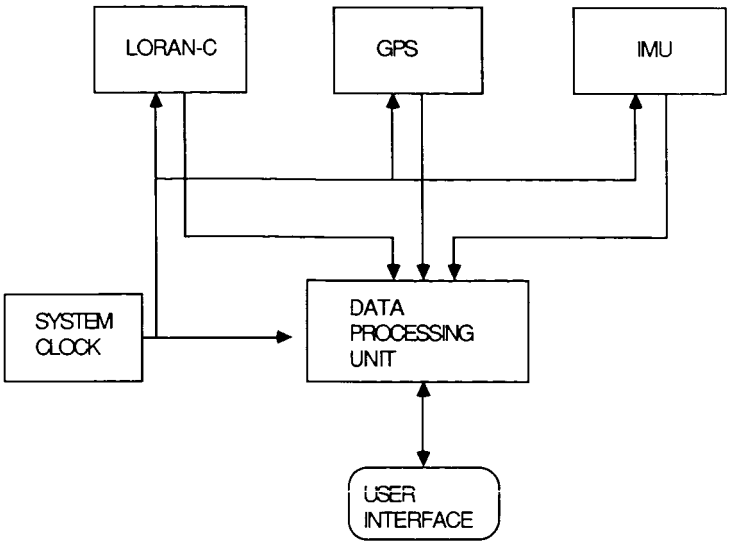

Figure 5. Integrated multisensor navigation system.

	NAVIGATION ACCURACY	
	SHORT TERM	LONG TERM
INS	GOOD TO EXCELLENT	POOR TO FAIR
GPS	FAIR TO POOR	EXCELLENT (VERY STABLE)
LORAN-C	FAIR TO POOR	GOOD (STABLE)
OMEGA	POOR TO BAD	FAIR
MLS	VERY GOOD	-------
ILS	GOOD	-------

Figure 6. Navigation system characteristics.

N87-27603

INVESTIGATION OF AIR TRANSPORTATION TECHNOLOGY AT PRINCETON UNIVERSITY, 1985

Robert F. Stengel
Department of Mechanical and Aerospace Engineering
Princeton University
Princeton, New Jersey

SUMMARY OF RESEARCH

The Air Transportation Technology Program at Princeton University, a program emphasizing graduate and undergraduate student research, proceeded along five avenues during 1985.

- Guidance and Control Strategies for Penetration of Microbursts and Wind Shear
- Application of Artificial Intelligence in Flight Control and Air Traffic Control Systems
- Use of Voice Recognition in the Cockpit
- Effects of Control Saturation on Closed-Loop Stability and Response of Open-Loop-Unstable Aircraft
- Computer-Aided Control System Design

Areas of investigation relate to guidance and control of commercial transports as well as general-aviation aircraft. Interaction between the flight crew and automatic systems is a subject of principal concern.

Recently, it has become apparent that severe downdrafts and resulting high-velocity outflows present a significant hazard to aircraft on takeoff and final approach. This condition is called a microburst, and while it often is associated with thunderstorm activity, it also can occur in the vicinity of dissipating convective clouds that produce no rainfall at ground level. Microburst encounter is a rare but extremely dangerous phenomenon that accounts for one or two air carrier accidents and numerous general aviation accidents each year (on average). Conditions are such that an aircraft's performance envelope may be inadequate for safe penetration unless optimal control strategies are known and applied. While a number of simulation studies have been directed at the problem, there are varied opinions in the flying community regarding the best piloting procedures, and optimal control strategies remain to be defined.

Graduate student Mark Psiaki has undertaken a study of guidance and control strategies for penetration of microbursts when

encounter is unavoidable. It has been shown that simple control laws could greatly reduce an aircraft's response to wind shear[1]. Although the response mechanism is the same, jet transport and general aviation aircraft behave somewhat differently in microbursts; the larger, heavier aircraft are more adversely affected by variations in the horizontal wind, while the smaller, lighter aircraft have greater difficulty with the downdraft.

Our emphasis has shifted to the determination of optimal control strategies for the microburst encounter[2]. The study has begun with the computation of optimal control histories using steepest-descent and second-order gradient algorithms. Once an envelope of safe flight has been determined for a typical jet transport, attention will be directed at a general aviation type, and optimal closed-loop control laws will be investigated. During the past year, a survey paper on the subject was published[3].

Undetected system failures and/or inadequately defined recovery procedures have contributed to numerous air carrier incidents and accidents. The infamous DC-10 accident at Chicago's O'Hare Airport, in which loss of an engine pod, subsequent loss of subsystems, and asymmetric wing stall led to disaster, provides a prototype for the kind of tragedy that could be averted by intelligent flight control systems. (An intelligent control system is one that uses artificial intelligence concepts, e.g., an expert systems program, to improve performance and fault tolerance.) Although many methods of modern control theory are applicable, the scope of the problem is such that none of the existing theories provides a complete and practical solution to the problem. At the same time, heuristic logic may be applicable, but it has yet to be stated in satisfactory format.

Graduate student David Handelman is developing a knowledge-based reconfigurable flight control system that will be implemented with the Pascal programming language using parallel microprocessors. This expert system could be considered a prototype for a fault-tolerant control system that could be constructed using existing hardware. Although funding for this effort has shifted to another source, results will have direct bearing on air transportation systems, as illustrated by [4]. In a parallel effort, graduate student Chien Huang is using the LISP programming language to investigate the utility of a string-oriented, recursive logical system in the same role. A principal distinction between this and the previous approach is that flight control code will be modified in response to control system failures.

Senior Takashi Sensui has begun to apply artificial intelligence principles in the study of air traffic control (Sensui, 1986). Working in the computer language PROLOG, he is designing optimal control logic for terminal area operations.

Prospects for reducing pilot workload through voice inputs to the aircraft are extremely promising, and graduate student Parvada Suntharalingam has completed a short study of the characteristics of a representative system (Suntharalingam, 1985). Using a commercially available system that is capable of recognizing continuous speech and which takes advantage of structured grammars, she demonstrated the effects of the number of training passes on misrecognition and rejection rates. Her results show that the system's errors are not greater than manual input errors of similar information.

One of the virtues of highly reliable electronic flight control systems is that an aircraft's stability and response, i.e., its closed-loop flying qualities, can be tailored to the pilot's needs. For reasons of performance and maneuverability, it may be desirable to design the aircraft so that its natural (unaugmented) modes of motion are unstable, with the understanding that the flight control system will provide the necessary stability by deflecting control surfaces to counter potentially divergent motions. Because control surfaces have limitations on their displacements and rates of travel, stability can be restored only within a bounded region about the trim point. If the aircraft's motions exceed the boundaries, the available control forces and moments will not be sufficient to prevent divergence.

Graduate student Prakash Shrivastava is developing methods for determining the stability boundaries and control response for systems containing control saturation[5,6]. Analysis is carried out using phase-plane plots, in which saturation and stability boundaries are represented by straight lines, stable trajectories approach equilibrium points, and unstable trajectories diverge to infinity. The analysis pertains to systems containing unequal saturation boundaries, as well as those with multiple saturating controls.

Future control-system engineers will benefit from design procedures that are computer-intensive, and it is important to create computer programs that allow designers to describe and analyze complex systems interactively. Senior Russell Nelson developed a control-system analysis program based on the LISP language mentioned above (Nelson, 1985). Analysis proceeds with classical concepts of transfer-function analysis in a program that can be run on a personal computer.

The FAA/NASA grant supporting student research in air transportation technology has inestimable value in helping educate a new generation of engineers for the aerospace industry, and it is producing research results that are relevant to the continued excellence of aeronautical development in this country.

1. Psiaki, M.L., and Stengel, R.F., "Analysis of Aircraft Control Strategies for Microburst Encounter", AIAA **Journal of Guidance, Control, and Dynamics**, Vol. 8, No. 2, Mar-Apr 1985, pp. 553-559.

Penetration of a microburst during takeoff or approach is an extreme hazard to aviation, but analysis has indicated that risks could be reduced by improved control strategies. Attenuation of flight path response to microburst inputs by elevator and throttle control was studied for a jet transport and a general aviation aircraft using longitudinal equations of motion, root locus analysis, Bode plots of altitude response to wind inputs, and nonlinear numerical simulation. Energy management relative to the air mass, a pitch-up response to decreasing airspeed, increased phugoid-mode damping, and decreased phugoid natural frequency were shown to improve microburst penetration characteristics. Aircraft stall and throttle saturation were found to be limiting factors in an aircraft's ability to maintain flight path during a microburst encounter.

2. Psiaki, M.L., and Stengel, R.F., "Optimal Flight Paths Through Microburst Wind Profiles", presented at the AIAA 12th Atmospheric Flight Mechanics Conference, Snowmass, CO, AIAA Paper No. 85-1833-CP, Aug 1985.

The problem of safe microburst wind shear encounter during the approach and climb-out flight phases was addressed using flight path optimization. The purpose was to investigate the physical limits of safe penetration and to determine control strategies that take full advantage of those limits. Optimal trajectories for both jet transport and general aviation aircraft were computed for encounters with idealized and actual microburst profiles. The results demonstrate that limits to control system design rather than to the aircraft's physical performance may be the deciding factor in an aircraft's capability for safe passage through a wide class of microbursts. The best control strategies responded to airspeed loss in an unconventional manner: by raising the nose to maintain lift.

3. Stengel, R.F., "Solving the Pilot's Wind-Shear Problem", **Aerospace America**, Vol. 23, No. 3, Mar 1985, pp. 82-85.

Although aircraft have had to contend with wind variability since the beginning of aviation, the July 1982 crash of Pan American Flight 759 on the outskirts of New Orleans, which killed 153 people, riveted attention on the hazards of flying in wind shear. Microbursts, unusually severe downdrafts

accompanied by intense outflows, prove especially hazardous during takeoff or landing. Within a minute or less the aircraft may be subjected to a headwind, then a downdraft, and then a tailwind. Just as the pilot throttles back to arrest ballooning above the nominal path caused by increase airspeed, headwind vanishes and downdraft causes the aircraft to lose lift. Lift is further degraded as the aircraft enters the outflow. A microburst compounded by heavy rain is thought to have caused the crash of Pan Am's Flight 759. The article addesses several aspects of the problem and proposes both short-term and long-term solutions.

4. Handelman, D.A., and Stengel, R.F., "Combining Quantitative and Qualitative Reasoning in Aircraft Failure Diagnosis", presented at the 1985 AIAA Guidance, Navigation, and Control Conference, Snowmass, CO, AIAA Paper No. 85-1905-CP, Aug 1985.

The problem of in-flight failure-origin diagnosis is addressed by combining aspects of analytical redundancy and artificial intelligence theory. The objective is to use a mathematical model of the aircraft's dynamic behavior to supplement the knowledge used for diagnosis. A method is developed whereby qualitative causal information about a dynamic system is drawn from its model. Based on sensitivities of the equations of motion to worst-case failure modes, a measure of the relative capacity of system elements to affect one another is derived. A diagnosis procedure combining problem reduction and backward-chaining ordered search uses this knowledge to reduce a list of elements capable of failure to a relatively small list of elements suspected of failure. Examples illustrate use of the knowledge base and the problem-solving mechanism that has been developed.

5. Shrivastava, P.C., and Stengel, R.F., "Stability Boundaries for Aircraft with Unstable Lateral-Directional Dynamics and Control Saturation", presented at the 1985 AIAA Guidance, Navigation, and Control Conference, Snowmass, Co, AIAA Paper No. 85-1948-CP, Aug 1985.

Aircraft that do not possess inherent (aerodynamic) stability must rely on closed-loop control systems for stable operation. Because there are limits on the deflections of an aircraft's control surfaces, the region of stable operation also is bounded. These boundaries were investigated for a lateral-directional example, in which vertical fin size was inadequate to provide directional stability and where aileron and rudder deflections were subject to saturation. Fourth-order models were used in this study, with flight control logic based upon minimum-control-energy linear-quadratic regulator theory. It was found that the stability boundaries can be described by

unstable limit cycles surrounding stable equilibrium points. Variations in regions of stability with gain levels and command inputs are illustrated. Current results suggest guidelines for permissible limits on the open-loop instability of an aircraft's lateral-directional modes.

6. Shrivastava, P.C., and Stengel, R.F., "Regions of Stability with Unequal Saturation Limits and Non-Zero Set Points", presented at the 24th IEEE Conference on Decision and Control, Fort Lauderdale, FL, IEEE Paper No. S-0128, Dec 1985.

Constraints on the magnitudes of control variables limit the region where open-loop unstable systems can be stabilized using feedback control. Variations in regions of stability with unequal control saturation limits and non-zero set points are illustrated for single-input unstable linear systems with one or two unstable eigenvalues. The regions of stability for saddle-point and unstable-node-type singularities increase in one of the saturation limits, but they become invariant when the larger control limit exceeds a certain value; the stability regions vanish for non-zero set points that saturate the controls. The unstable-focus-type singularity exhibits strikingly different characteristics. These results suggest guidelines for obtaining desired stability regions for different types of singularities.

ANNOTATED BIBLIOGRAPHY

1. Nelson, R.F., "Computer Aided Control System Design", Princeton University Independent Work Report, May 1985.

The objectives of this project were to develop an interactive computer program to serve as a tool in the design of control systems and to evaluate the utility of the LISP programming language in this application. An environment of LISP functions that allows the user to define and examine a system characterized in the frequency domain was developed. The program generates a block diagram of a multiloop system, then computes frequency-response characteristics between arbitrary points in the diagram; these can be displayed as Bode or Nyquist plots. The LISP language was found to provide a flexible, interactive tool that could aid the development of large-scale systems.

2. Sensui, Takashi, "Automation of the Terminal Area Air Traffic Control System - Progress Report", Princeton University Independent Work Report, Jan 1986.

The objective of the project is to design logic for a fully automated terminal area control system. Design specifications have been defined, and application of an expert system is discussed. A brief comment concerning the programming of simplified models is included.

3. Suntharalingam, P., "A Test on the Reliability and Performance of the Verbex Series 4000 Voice Recognizer", Internal Memorandum, Princeton University Laboratory for Control and Automation, Sept 1985.

Speech input is becoming an increasingly important form of data entry. The object of this exercise was to test and explore the features of a voice recognition unit that enables communication between human and machine. The unit is speaker-dependent, i.e., it requires training with a given vocabulary as spoken by a single person. The speaker's voice patterns are stored on a solid-state cartridge and are subsequently used as templates for recognition. Two additional features of the unit are its ability to recognize continuous speech (strings of words as opposed to single commands) and its use of structured grammars, in which words of specified classes (subject, predicate, modifier, etc.) must be spoken in a fixed order. Tests were run to determine the voice recognition unit's error rates as functions of machine training level and to determine the relative merits of structured and unstructured grammars. It was found that error rates varied from one speaker to the next; some speakers required more training passes than others to achieve a given level of recognition accuracy. It also was noted that a structured grammar requires less training than an unstructured one to achieve a given accuracy. However, the latter may be preferred for its greater flexibility; with sufficient training, the error rates may be reduced to acceptable levels.

OPTIMIZATION OF AIRCRAFT TRAJECTORIES THROUGH SEVERE MICROBURSTS

Mark L. Psiaki
Department of Mechanical and
Aerospace Engineering
Princeton University
Princeton, NJ

PERFORMANCE ENVELOPES, MICROBURST PENETRATION

A method of defining performance envelopes for aircraft microburst penetration is being developed. A trajectory is computed for a given aircraft/control law configuration and given microburst parameters (either a downdraft or a head/tailwind type microburst). The maximum deviation from the nominal altitude is recorded for that trajectory. Then the microburst parameters are varied, and the process is repeated. Thus a three-dimensional plot of maximum altitude deviation versus microburst range scale and intensity is generated. Finally, a certain maximum altitude deviation, say 50 feet, is defined as the safe penetration limit. Then the 50 foot level contour becomes the performance limit for safe operation as a function of microburst intensity and range.

Control inputs from deterministic trajectory optimization are used in the above described calculations to define the maximal (least conservative for a given airframe/power plant) performance limit. These limits provide targets for the designer of practical control laws. A practical control law with microburst performance limits near the maximal limits is a good control law from this standpoint.

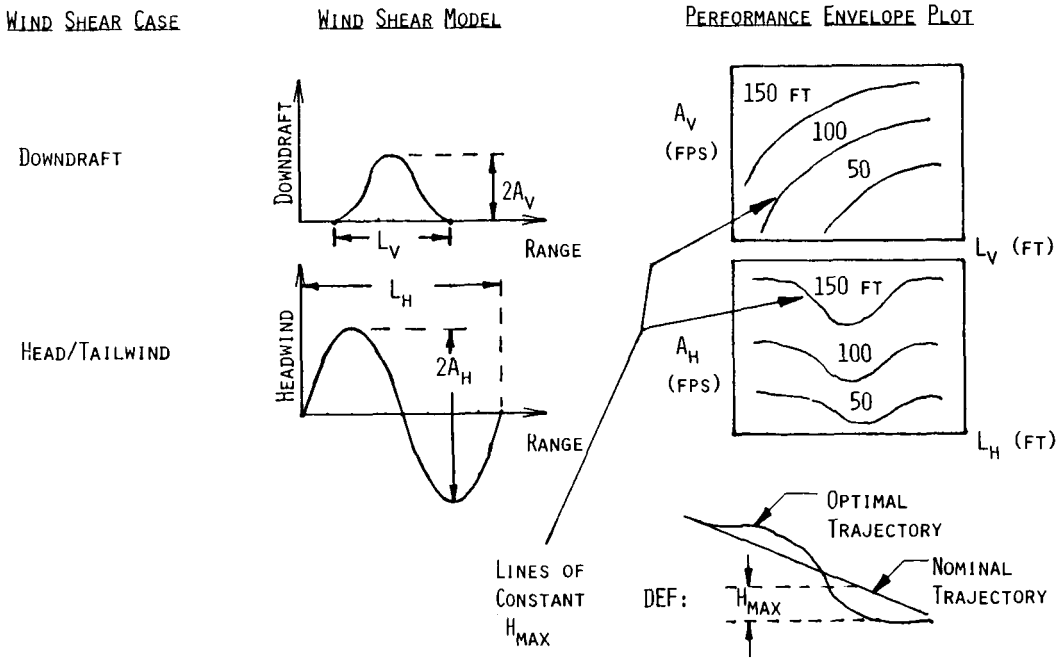

WORK PERFORMED SINCE SEPTEMBER 1985

During the past four months work has been done in four areas. At first attempts were made to develop faster optimization procedures for use with the full-nonlinear-aerodynamics General Aviation (GA) model. Next, efforts were made towards generating the maximal performance envelopes for the Jet Transport model. Batch software for the IBM PC-XT was needed to do this efficiently. Each trajectory optimization takes 1 to 2 hours. The batch software allows one PC to do 10 or more optimizations overnight. The first of several iterations began by attempting to calculate maximal performance envelopes, having the optimization algorithm run into difficulties, and finding a fix for the difficulties. In the process two major changes to the optimization algorithm were incorporated. One was a switch from numerical to analytical evaluation of the sensitivities of the discrete-time optimization problem. The other eliminated the penalty function formulation of the control saturation and stall limit inequality constraints. It was replaced by a Lagrange multiplier formulation with a modified Newton's method search procedure.

- ATTEMPT TO SPEED UP NAVION MODEL OPTIMIZATION
- GENERATION OF MULTI-OPTIMIZATION BATCH SOFTWARE
- ATTEMPTS TO CALCULATE BOEING 727 MAXIMAL PERFORMANCE ENVELOPES
- OPTIMIZATION PROCEDURE IMPROVEMENTS

  ANALYTIC DERIVATIVES OF DISCRETE-TIME SYSTEM

  LAGRANGE MULTIPLIER FORMULATION OF INEQUALITY CONSTRAINTS. EXTENSION OF NEWTON'S METHOD

ANALYTIC DERIVATIVES OF DISCRETE-TIME SYSTEM

The problem was transformed into discrete-time form in order to solve the deterministic trajectory optimization on a digital computer. The discrete-time nonlinear difference equation was generated from the continuous-time differential equation by numerically solving the initial value problem (I.V.P.) shown under the definition of the difference equation's right hand side (RHS).

First and second derivatives of the RHS of the difference equation and the cost function are needed in order to do trajectory optimization using Newton's method. Previously these derivatives had been calculated numerically using a three-point scheme. When microburst intensities got large, problems cropped up in the convergence of the optimization algorithm near the solution. A simple example showed that roundoff error in numerical differentiation could be the cause. When analytic derivatives were substituted the problem went away.

The analytic derivatives of the nonlinear difference equation were generated as follows: The RHS of the difference equation is defined as the solution of an I.V.P. At each instant of time the solution to the I.V.P. depends on the arguments of the RHS of the difference equation. Differentiation of the I.V.P. -- both initial conditions and differential equation -- any number of times with respect to the arguments of the difference equation yields a new I.V.P. This new I.V.P. might be a matrix or a tensor I.V.P. depending on the number of differentiations. It, too, can be solved numerically to yield the corresponding derivative of the RHS of the difference equation.

- DEFINITION: $\underline{x}_{K+1} = \hat{\underline{E}}(\underline{x}_K, \underline{u}_K, K)$

  WHERE $\hat{\underline{E}}(\underline{x}_K, \underline{u}_K, K) = \underline{x}(\tau_{K+1})$, $\underline{x}(\tau)$ THE SOLUTION

  OF THE I.V.P.

  $$\dot{\underline{x}}(\tau) = \underline{E}[\underline{x}(\tau), \underline{u}_K, \tau]$$
  $$\underline{x}(\tau_K) = \underline{x}_K$$

- EXAMPLE DISCRETE TIME SENSITIVITY (DIFFERENTIATE THE I.V.P.):

  $$\frac{\partial \hat{\underline{E}}}{\partial \underline{x}_K} = \frac{\partial \underline{x}(\tau_{K+1})}{\partial \underline{x}_K} \text{ , } \frac{\partial \underline{x}(\tau)}{\partial \underline{x}_K} \text{ THE SOLUTION}$$

  OF THE I.V.P. $$\frac{D}{D\tau}\left(\frac{\partial \underline{x}(\tau)}{\partial \underline{x}_K}\right) = \frac{\partial \underline{E}}{\partial \underline{x}}[\underline{x}(\tau), \underline{u}_K, \tau]\frac{\partial \underline{x}(\tau)}{\partial \underline{x}_K}$$

  $$\frac{\partial \underline{x}(\tau_K)}{\partial \underline{x}_K} = I$$

TRAJECTORY OPTIMIZATION WITH INEQUALITY CONSTRAINTS

The optimization problem with inequality constraints is one of picking a control time history, u(k) for k = 1...N-1 which minimizes the cost, J, subject to the discrete-time plant difference equation and the discrete-time inequality constraints. Inequality constraints can be used to deal with control saturation and to limit the angle of attack to be below stall. Proper handling of control saturation and the stall limit is essential to maximal performance envelope determination.

This optimization problem can be solved by the penalty function method. A penalty cost is added to L whenever one of the inequality constraints is violated. With this modified cost function, an unconstrained optimal trajectory is determined. As the penalty is increased, the solution approaches that of the original problem. In practice there is a limit to how fast the penalty cost can be increased. Many unconstrained optima must be computed before an answer sufficiently close to the constrained optimum is attained.

Direct necessary conditions for the inequality-constrained optimum are attributed to Kuhn and Tucker *. According to these necessary conditions, the inequality constraints are ignored when the optimal solution satisfies them but does not lie on the boundary. The constraint is treated as an equality constraint when the optimal solution does lie on the boundary. Then the Lagrange multipliers must be non-negative, so that no better solution lies in the admissible region. An extension of Newton's method is used to search for a solution to the necessary conditions. These conditions are linearized about the current guess. Then a quadratic programming problem is solved to get the next guess for the optimal time histories. This procedure yields "exact" solutions to the inequality-constrained problem in as much time as is required to solve an unconstrained problem, reducing computation by a factor of three or more from the penalty function method.

The quadratic programming algorithm so far implemented to determine the extended Newton's method increment has proven to be less than fully reliable. Therefore, a new algorithm has been identified and is under development.

* Luenberger, D.G., *Optimization by Vector Space Methods*, John Wiley and Sons, (New York, 1969), pp. 247-253.

TRAJECTORY OPTIMIZATION WITH INEQUALITY CONSTRAINTS

PROBLEM: MINIMIZE $$J = \sum_{K=1}^{N-1} L(\underline{x}_K, \underline{u}_K, K) + V(\underline{x}_N)$$

SUBJECT TO: $$\underline{x}_{K+1} = \hat{\underline{F}}(\underline{x}_K, \underline{u}_K, K) \qquad K = 1....N-1$$

$$\underline{x}_1 \text{ GIVEN}$$

$$\underline{C}(\underline{x}_K, \underline{u}_K, K) \leq 0 \qquad K = 1....N-1$$

PENALTY FUNCTION METHOD: ADD COST TO $L(\underline{x}_K, \underline{u}_K, K)$ IF CONSTRAINT IS VIOLATED

LAGRANGE MULTIPLIER METHOD: TREAT INEQUALITY CONSTRAINT AS EQUALITY CONSTRAINT IF BETTER SOLUTION VIOLATES CONSTRAINT, OTHERWISE IGNORE CONSTRAINT.

OPTIMAL TRAJECTORIES THROUGH SEVERAL MICROBURSTS

Six of the many optimal trajectories so far calculated are displayed on this graph. These six are all Jet Transport take-off trajectories through 10,000 ft. microbursts. The engineering approximation microbursts have only longitudinal winds: the head/tailwind varies as one period of 10,000 ft. sine wave. The arrows represent the relative wind magnitudes and directions. The six different curves represent optimal trajectories for the same cost function (a cost function which weights altitude deviations from the nominal most highly) and six different wind intensities. At the highest intensity, 120 fps maximum head/tailwind (240 fps longitudinal wind differential in 5,000 ft)., the maximum altitude deviation reaches 200 ft. Appreciable maximum altitude deviations (greater than 40 ft.) occur at microburst intensities above 100 fps maximum head/tailwind.

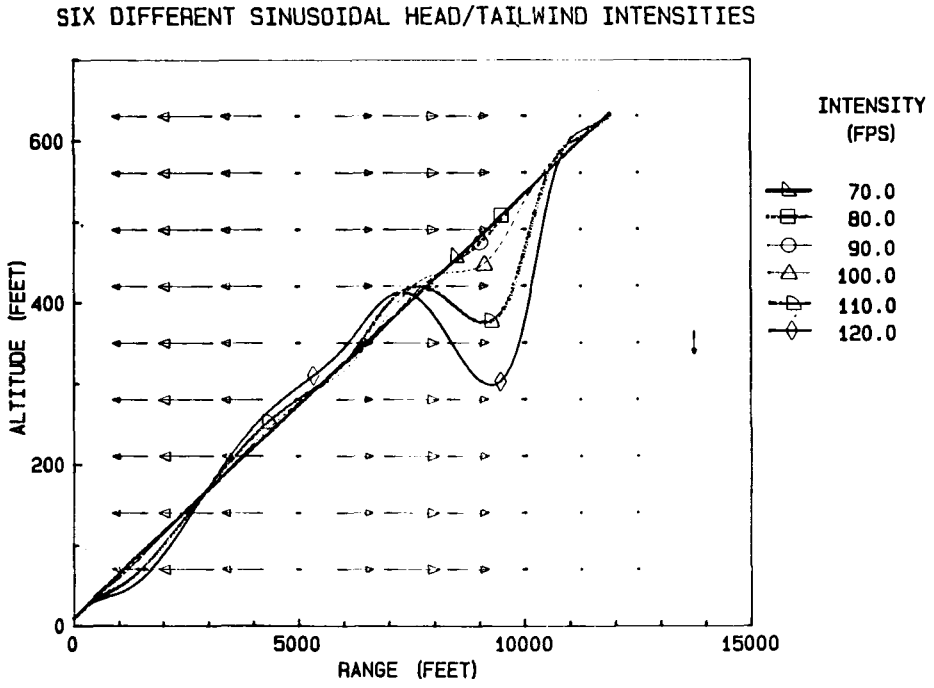

TAKE-OFF THROUGH SEVERAL MICROBURSTS

Time (range) histories of throttle setting, airspeed, angle of attack and elevator angle are shown. Several features are noteworthy:

1. Full throttle is not commanded until some time after the beginning of the optimization for the three microbursts of lowest intensity. Full throttle is commanded immediately upon initiation of the optimization for the other three cases. Maximum altitude deviation is significant in the latter three cases. The optimization would have anticipated the microburst by commanding full throttle even earlier if it could have done so. Thus, the degree to which any controller can anticipate the airspeed loss due to a microburst directly relates to the degree of flight path tracking.

2. In those cases where airspeed fell below the 1-g stall limit, the angle of attack was raised to the stall boundary at approximately the same time. Subsequent regaining of airspeed margin above stall, however, did not dictate coincident lowering of angle of attack below the stall. Rather, the angle of attack remained at its stall limit for some time after sufficient airspeed was regained for trim at the nominal flight path angle. This was necessary to regain altitude lost during the period of airspeed deficiency. The fact that stall angle of attack did not precede stall airspeed indicates little or no microburst anticipation in the optimal pitch steering scheme. Therefore, near optimal, practical (causal) pitch steering may be possible.

3. The plots of elevator angle indicate that constant stall angle of attack can only be maintained through a varying command. The pilot has to manuever to stay at this angle of attack.

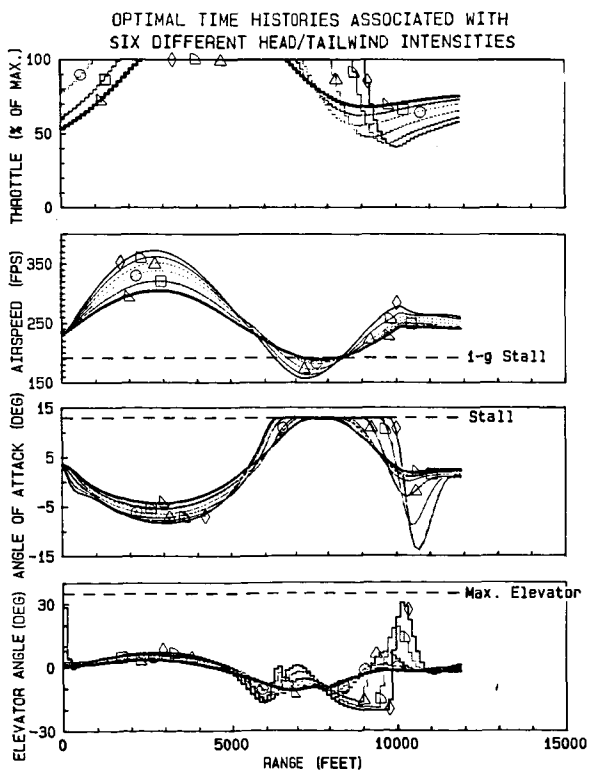

TAKE-OFF TRAJECTORY TRACKING PERFORMANCE OF A JET TRANSPORT

The plot to the left on this figure shows actual results for maximal microburst penetration performance during take-off of a Boeing-727. The microbursts under consideration were the head/tailwind sine wave type. Each triangle on the plot indicates an actual data point: for each triangle, an optimization was run through a sinusoidal head/tailwind microburst of the corresponding range and intensity, and the maximal altitude deviation from nominal was recorded. Contours of equal maximum altitude deviation were then generated via linear interpolation (extrapolation in one case) in the microburst intensity direction and parabolic curve fitting in the microburst range direction. The minima of the three upper contours occurred at microburst range scales near that of the open-loop phugoid mode. If the plot on the left were a three dimensional (3D) plot of maximal altitude deviation (positive out of the paper) versus microburst range and intensity, then the plot to the right would be the cross section of the 3D plot taken at the microburst range 10,000 ft. The "knee" in this curve corresponds to the microburst intensity where full throttle is commanded at the beginning of optimization.

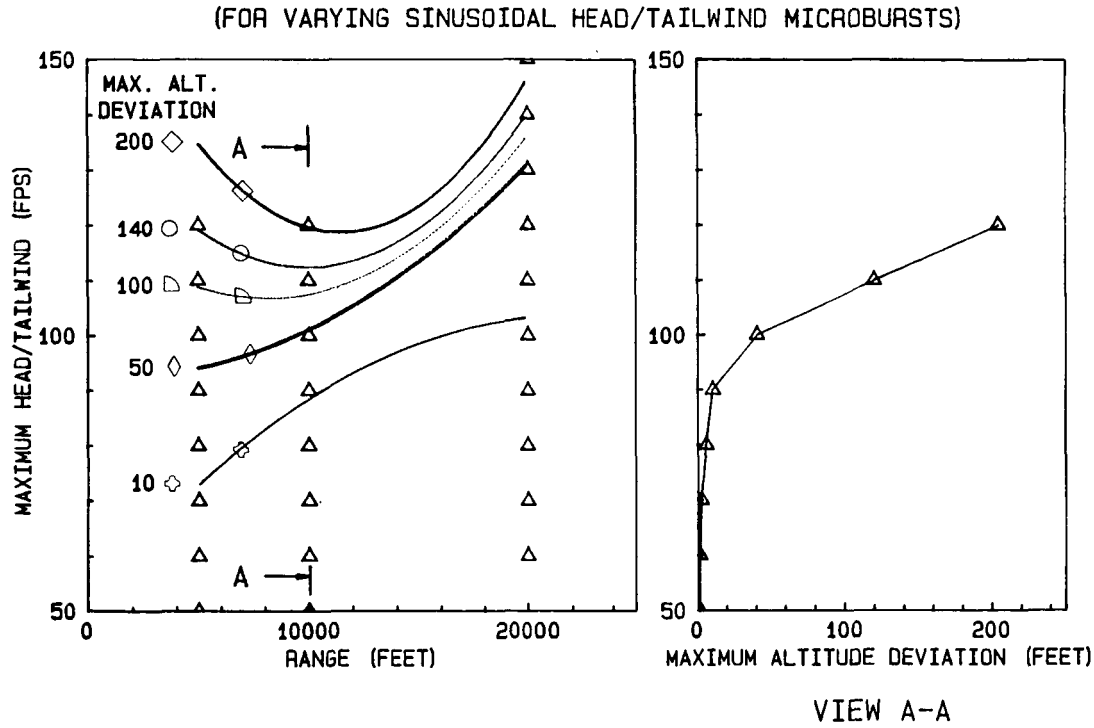

CONCLUSIONS

The improvements to the nonlinear deterministic trajectory optimization algorithm were significant. The use of analytic derivatives solved some numerical problems. The extension of Newton's method to handle inequality constraints may represent an important contribution to the general field of deterministic trajectory optimization. In any case, it contributed greatly to the feasibility of doing the performance envelope calculations at hand, reducing computation time by a factor of three and higher. What would have taken 3 hours on the IBM 3081 a year ago now takes 1.5 hours on an IBM PC-XT.

Examination of optimal trajectories through extreme microbursts and the strategies employed to achieve them shed light on the control problem. A relationship was found between anticipatory throttle activity and the ultimate maximum altitude deviation. Therefore, the ultimate performance of an optimized trajectory will depend significantly upon the point at which one chooses to begin optimization. In order to normalize for this effect, we chose to begin our optimizations at the leading edge of each microburst. The optimal angle of attack strategy showed a close correspondence to the optimal airspeed policy with little anticipation, so it seems feasible to develop a controller that would vary angle of attack to minimize the effect of airspeed variations upon lift up to the stall saturation limit, at which point it would hold the stall angle of attack until the aircraft was well on the way to recovery.

- TRAJECTORY OPTIMIZATION ALGORITHM

  UNIQUENESS AND EFFECTIVENESS OF NEWTON'S METHOD APPLIED TO INEQUALITY CONSTRAINTS

  FEASIBILITY OF MAXIMAL PERFORMANCE ENVELOPE CALCULATIONS

- OPTIMAL MICROBURST PENETRATION

  DEPENDENCE UPON INITIAL RANGE

  ANTICIPATION THROTTLE STRATEGY

  FEASIBILITY OF ANGLE OF ATTACK STRATEGY

PLANNED FUTURE WORK

The first task is to finish development of the new optimization procedure, especially the quadratic programming portion of the extended Newton's method. Hildreth's quadratic programming procedure * adapted to use the Conjugate Gradient method should yield an efficient and robust algorithm. The GA model still needs to be worked in with the new optimization procedure in order to calculate GA performance envelopes. As software is developed performance envelopes will be calculated for downdraft type and head/tailwind type microbursts, landing and take-off flight phases, and Jet Transport and General Aviation type aircraft. As time permits, practical control laws will be developed which approach the performance of deterministic optimal microburst penetration.

* Luenberger, D.G., *Optimization by Vector Space Methods*, John Wiley and Sons, (New York, 1969), pp. 299-300.

- OPTIMIZATION ALGORITHM
  - PERFECT QUADRATIC PROGRAMMING PORTION OF NEWTON'S METHOD
  - GET NAVION MODEL WORKING
- PERFORMANCE ENVELOPE CALCULATIONS
  - BOEING 727 AND NAVION AIRCRAFT
  - LANDING AND TAKE-OFF PHASES
  - HEAD/TAIL WIND AND DOWNDRAFT TYPE MICROBURSTS
- PRACTICAL CONTROL LAW DESIGN

FAULT-TOLERANT FLIGHT CONTROL SYSTEM COMBINING EXPERT SYSTEM AND ANALYTICAL REDUNDANCY CONCEPTS

Dave Handelman
Department of Mechanical and Aerospace Engineering
Princeton University
Princeton, New Jersey

PROBLEM DEFINITION

This research involves the development of a knowledge-based fault-tolerant flight control system. The objective is to design a control system capable of accommodating a wide range of time-critical aircraft failures, including actuator, sensor, and structural failures. A software architecture is presented that integrates quantitative analytical redundancy techniques and heuristic expert system problem-solving concepts for the purpose of in-flight, real-time failure accommodation.

The overall job of failure accommodation is broken down into five main tasks: executive control, failure detection, failure diagnosis, failure model estimation, and reconfiguration. The executive control task provides continual dynamic state estimation, feedback control calculations, and synchronization of the remaining tasks. The failure detection task monitors aircraft behavior and detects significant abnormalities. Failure diagnosis finds a list of aircraft components most likely to have caused the problem, while the failure model estimation task generates a mathematical model of the aircraft dynamics that reflects changes due to the failure. Finally, the reconfiguration task determines what action should be taken to correct the situation.

In order to carry out its assigned tasks, the control system uses as building blocks powerful analytical techniques developed within the state-space environment of modern control theory. For example, the executive control task employs a Kalman Filter and a Linear-Quadratic Regulator for estimation and control. Innovation-based and Multiple Model algorithms are used in failure detection and failure model estimation, respectively. Additionally, a weighted left pseudo-inverse procedure is available for reconfiguration if needed. These quantitative methods provide effective solutions to certain aspects of the failure accommodation problem.

Because they are computationally intensive, however, these algorithms must be used judiciously if real-time fault-tolerance ultimately is to be achieved. Efficient scheduling and selection of tasks and subtasks thus becomes an overriding control system design factor. Moreover, these quantitative algorithms do not reflect the type of problem solving performed by pilots. For these reasons, the control system will benefit from the incorporation of a qualitative, heuristic reasoning capability. The research described here uses artificial intelligence techniques to combine the strengths of quantitative and qualitative reasoning for fault-tolerant flight control.

FAILURE ACCOMMODATION TASK SAMPLE

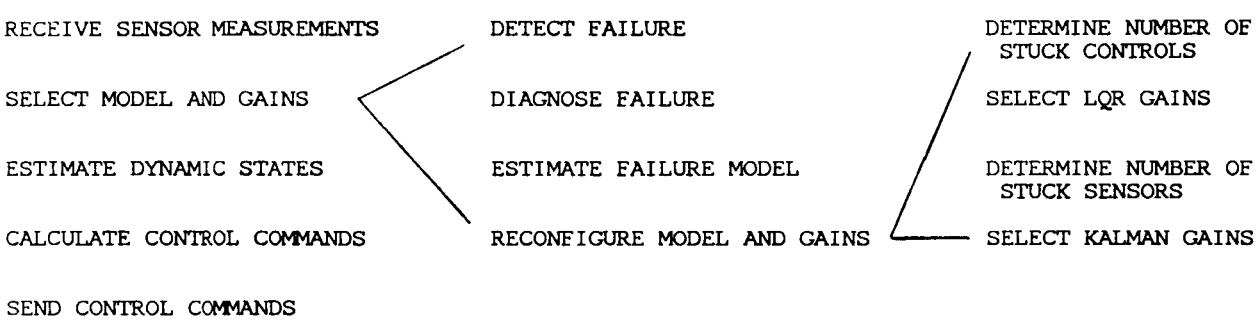

EXPERT SYSTEM DESCRIPTION

A rule-based backward-chaining expert systems approach is used to transform the problem of failure accommodation into a problem of search. The expert system is composed of a knowledge base and an inference engine. The knowledge base contains parameters that represent important variables and rules that relate parameters in the form of IF <PREMISE> THEN <ACTION> clauses.

EXECUTIVE CONTROL KNOWLEDGE BASE SAMPLE

RULE-E02	IF	CONTROL COMMANDS ARE CALCULATED
	THEN	SEND CONTROL COMMANDS.
RULE-E04	IF	TRIM CONTROL COMMANDS ARE CALCULATED AND PERTURBATION CONTROL COMMANDS ARE CALCULATED
	THEN	CALCULATE CONTROL COMMANDS.
RULE-E07	IF	MODEL, CONTROLLER, AND ESTIMATOR ARE READY AND DYNAMIC STATES ARE ESTIMATED
	THEN	CALCULATE PERTURBATION CONTROL COMMANDS.
RULE-E08	IF	MODEL, CONTROLLER, AND ESTIMATOR ARE READY AND SENSOR MEASUREMENTS ARE RECEIVED
	THEN	ESTIMATE DYNAMIC STATES.
RULE-E09	IF	THIS RULE IS BEING TESTED
	THEN	RECEIVE SENSOR MEASUREMENTS.
RULE-E10	IF	RECONFIGURATION IS NOT REQUESTED
	THEN	MODEL, CONTROLLER, AND ESTIMATOR ARE READY.

EXECUTIVE CONTROL KNOWLEDGE BASE
(PART I)

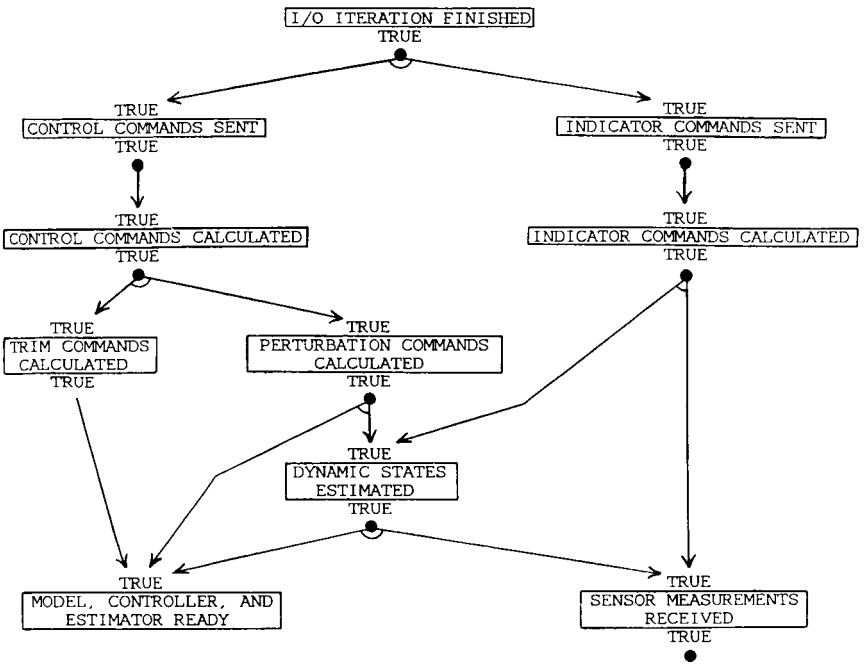

EXECUTIVE CONTROL KNOWLEDGE BASE
(PART II)

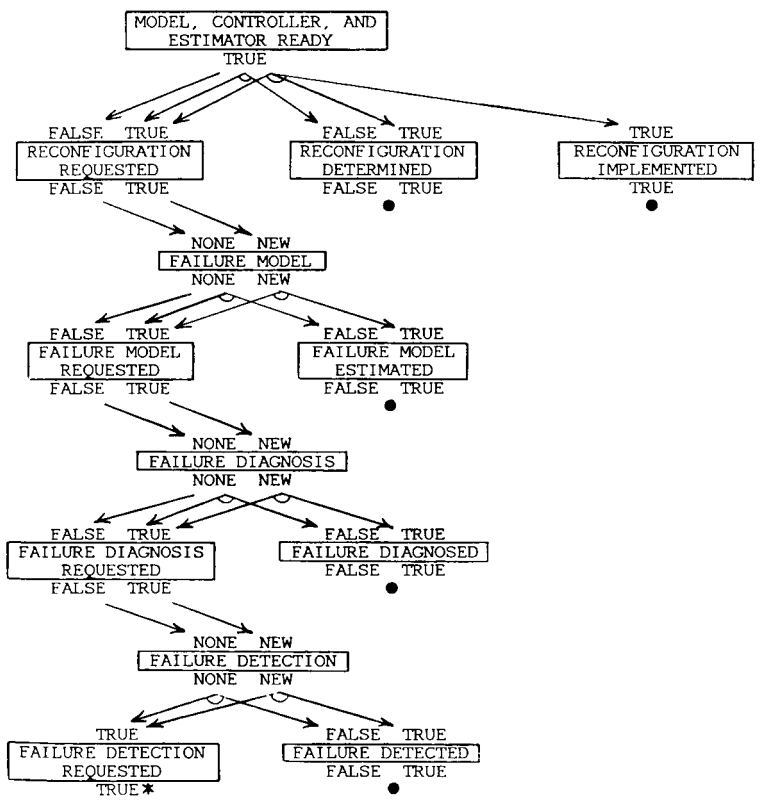

THE INFERENCE ENGINE

The inference engine applies a given set of rules to problem-specific data assigned to parameters. With all non-initialized parameter values assumed unknown, the act of trying to infer the value of a parameter, such as I/O-ITERATION-FINISHED, begins the search process. The estimation, control, and analytical redundancy algorithms reside as procedures in the actions of relevant rules, being executed when needed during the search. Presently, the knowledge base contains nearly 80 parameters and over 100 rules.

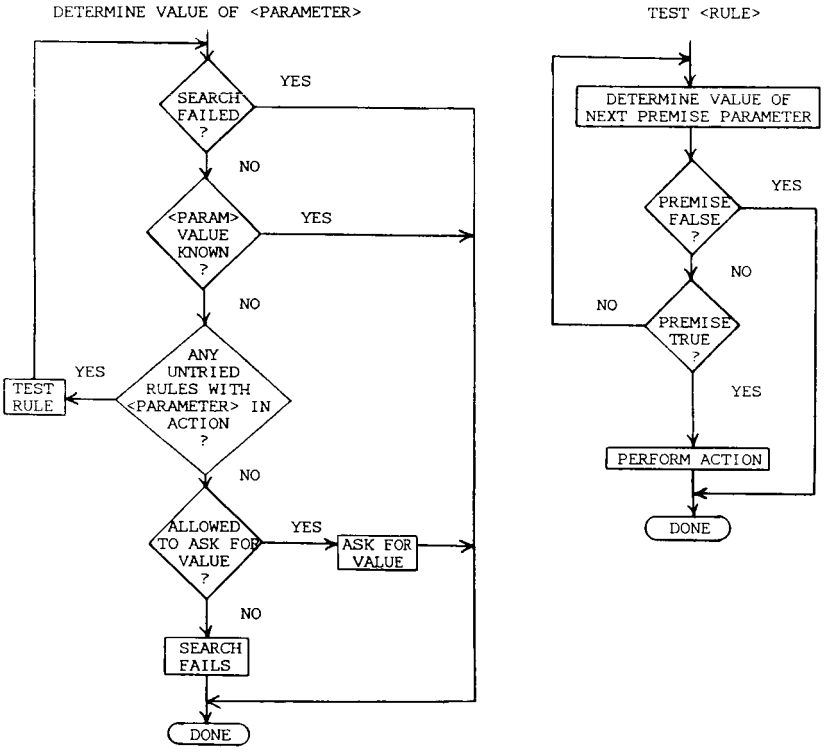

KNOWLEDGE BASE CONTENTS

TASK	PARAMETERS	RULES	MAJOR SUBTASKS
EXECUTIVE CONTROL	23	31	KALMAN FILTER LINEAR QUADRATIC REGULATOR
FAILURE DETECTION	8	12	NORMALIZED INNOVATIONS MONITOR
FAILURE DIAGNOSIS	2	1	SIGNAL DEPENDENCY SEARCH (TO BE INCLUDED)
FAILURE MODEL ESTIMATION	14	20	MULTIPLE MODEL ALGORITHM
RECONFIGURATION	31	37	LEFT PSEUDO-INVERSE

CH-47 CONTROL VECTOR DEFINITION

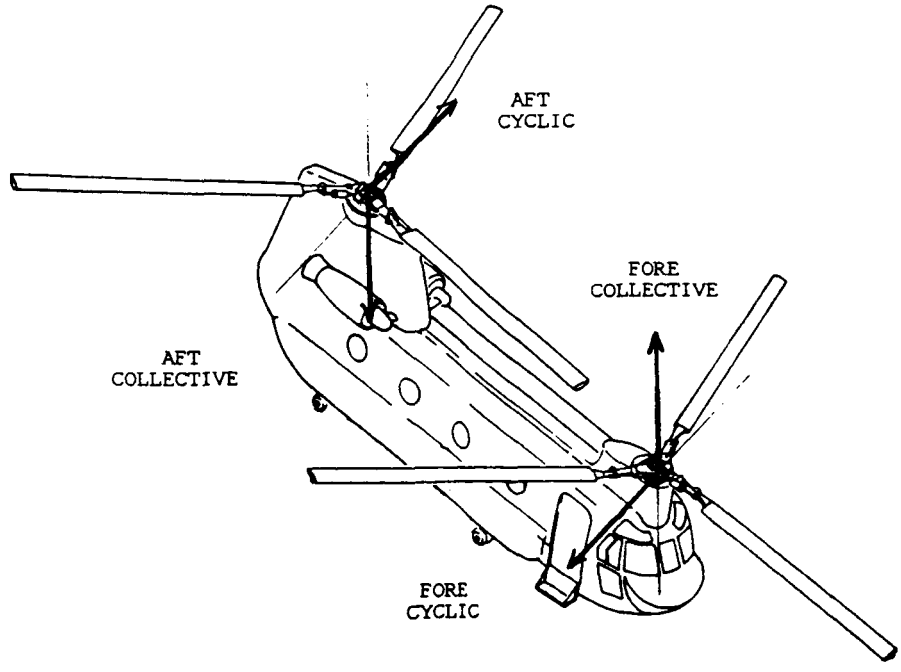

SIMULATION RESULTS

Control system performance is evaluated through ground-based simulations of in-flight failures. Using a linear discrete deterministic dynamic model of a Boeing CH-47 tandem-rotor helicopter, the effect of biased and stuck sensors and controls is investigated.

Failures are injected into the aircraft model at the 1.0 sec point of the simulation. When a sliding average of the nominal estimator normalized tracking error exceeds a preset threshold, the control system declares that a failure exists. Because rules for autonomous failure diagnosis and failure model hypothesis generation have yet to be included, the control system is given four failure model hypotheses at the end of time allotted for diagnosis. These hypotheses, to be used in the failure model estimation Multiple Model Algorithm, include the hypothesis representing no failure, the hypothesis representing the actual failure, and two hypotheses reflecting half and double the actual failure mode specification.

In order to simulate eventual parallel processing on a single-processor computer, the asynchronous tasks of failure diagnosis and reconfiguration are artificially delayed 0.5 sec each, thus simulating 0.5 sec task completion times. Executive control, failure detection, and failure model estimation, on the other hand, are all designed to cycle through one full search per sampling interval, and therefore incur no artificial delay.

The scheduling and selection of quantitative tasks occurs inherently within the expert system search process. A measure of the amount of search effort required to accomplish this scheduling and selection is indicated by the number of rules tested versus the number of parameters set during the search. Prior to beginning the search, all parameters without an initial value are assumed unknown. Rules are tested in an effort to set parameters, ultimately setting the top-level goal parameter. With a normalized search workload defined as the number of rules tested divided by the number of parameters set, it can be seen that tasks stressing selection over scheduling incur a higher workload, representing a lower search efficiency.

SIMULATED ACCOMMODATION OF BIASED CONTROL: LONGITUDINAL STATE & CONTROL TIME HISTORIES

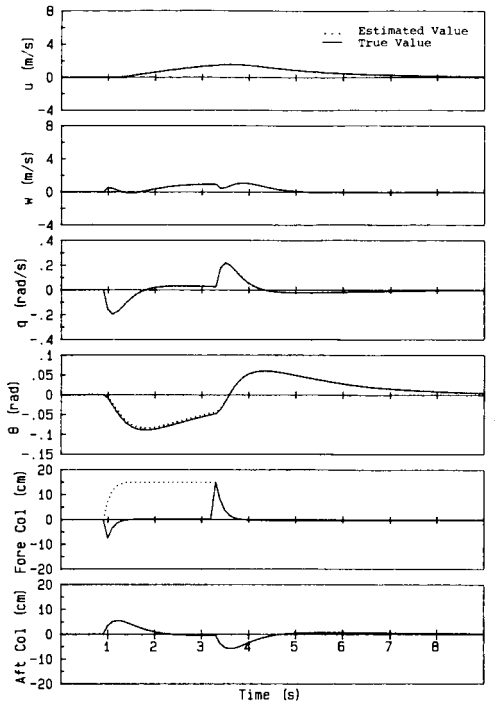

Forward Collective Pitch Control Biased 15 cm @ t=1.0s

SIMULATED ACCOMMODATION OF BIASED CONTROL: FAILURE DETECTION AND FAILURE MODEL ESTIMATION SEARCH RESULT TIME HISTORIES

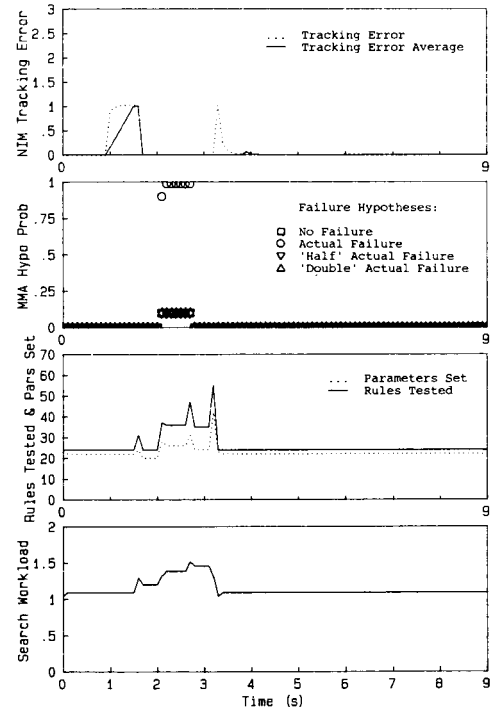

Forward Collective Pitch Control Biased 15 cm @ t=1.0s

SIMULATED ACCOMMODATION OF BIASED SENSOR: LONGITUDINAL STATE & CONTROL TIME HISTORIES

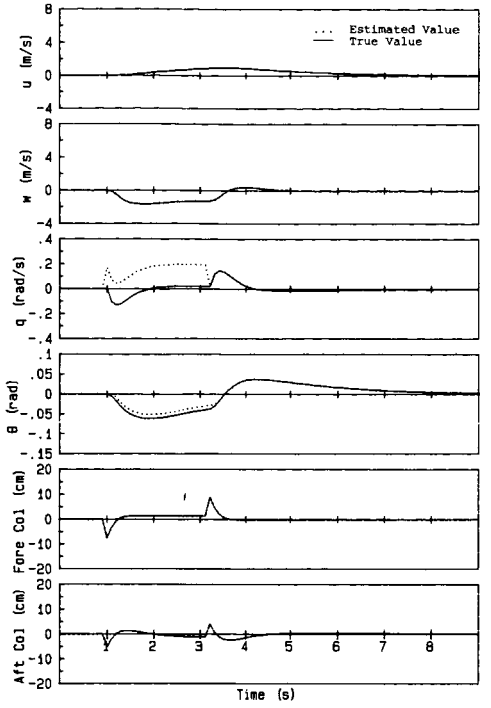

Pitch Rate Sensor Biased 0.18 rad/s @ t=1.0s

SIMULATED ACCOMMODATION OF BIASED SENSOR: FAILURE DETECTION & FAILURE MODEL ESTIMATION SEARCH RESULT TIME HISTORIES

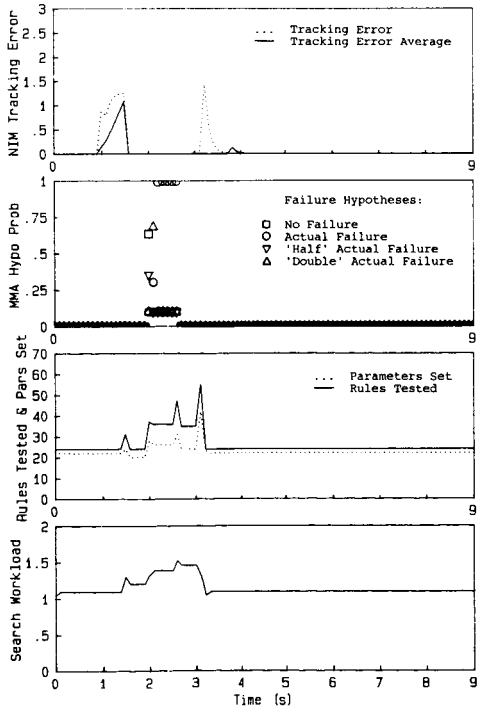

Pitch Rate Sensor Biased 0.18 rad/s @ t=1.0s

SIMULATED ACCOMMODATION OF STUCK CONTROL LONGITUDINAL STATE & CONTROL TIME HISTORIES

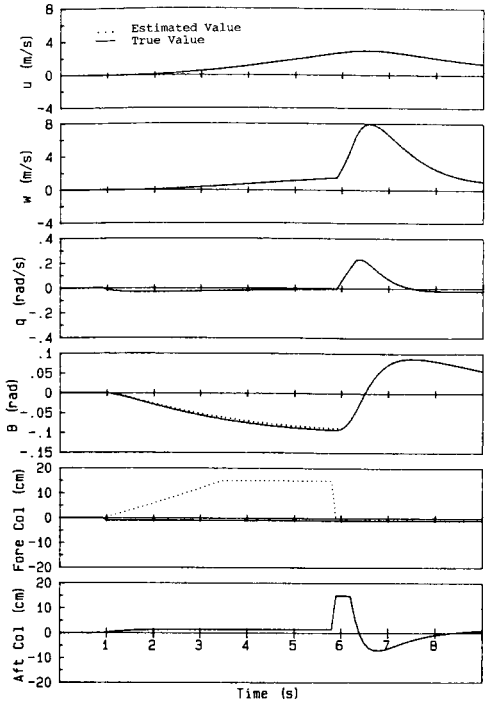

Forward Collective Pitch Control Stuck 1 cm from Nominal @ t=1.0s

SIMULATED ACCOMMODATION OF STUCK CONTROL: FAILURE DETECTION & FAILURE MODEL ESTIMATION SEARCH RESULT TIME HISTORIES

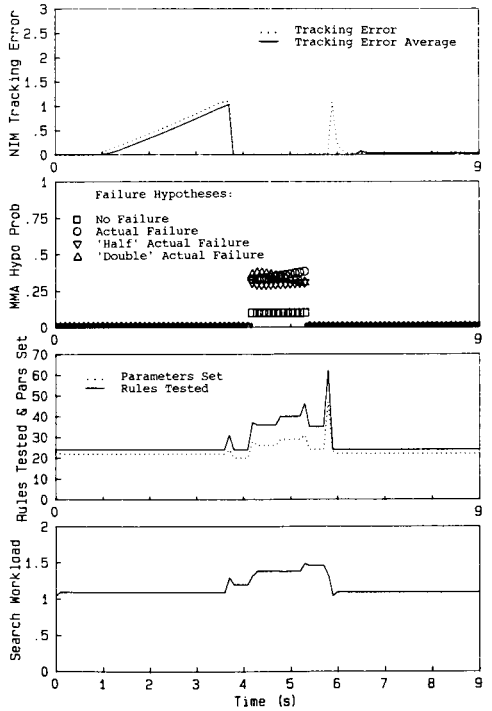

Forward Collective Pitch Control Stuck 1 cm from Nominal @ t=1.0s

SIMULATED ACCOMMODATION OF STUCK SENSOR: LONGITUDINAL STATE & CONTROL TIME HISTORIES

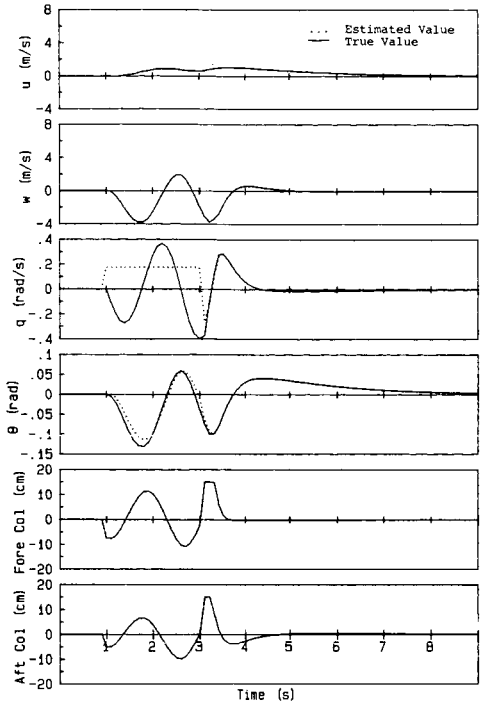

Pitch Rate Sensor Stuck 0.18 rad/s from Nominal @ t=1.0s

SIMULATED ACCOMMODATION OF STUCK SENSOR: FAILURE DETECTION & FAILURE MODEL ESTIMATION SEARCH RESULT TIME HISTORIES

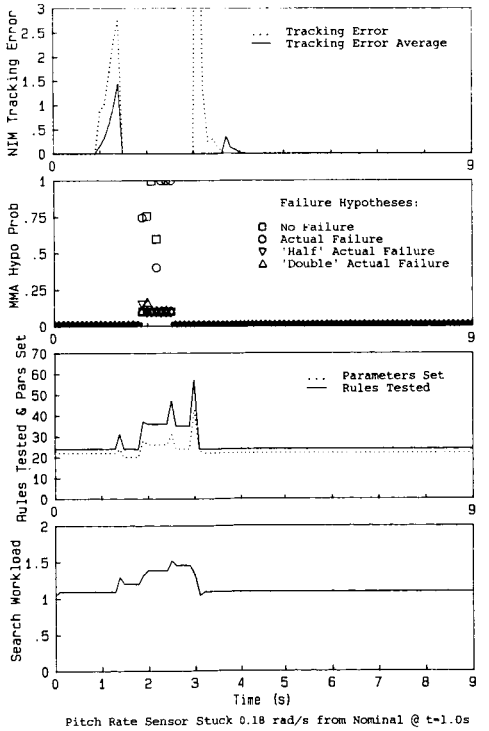

Pitch Rate Sensor Stuck 0.18 rad/s from Nominal @ t=1.0s

RESPONSE TO FALSE ALARM

A failure detection mechanism should be sensitive to dynamic abnormalities, yet have a low false alarm rate. Should a false alarm occur, however, the control system must be able to recognize that a mistake has been made without compounding the problem. Simulations producing a false alarm immediately following reconfiguration for a stuck sensor demonstrate this ability in the proposed control system. By estimating the failure model to be the one corresponding to the no-failure hypothesis, the expert system recognizes the mistake and effectively suppresses any improper corrective action that might have otherwise taken place.

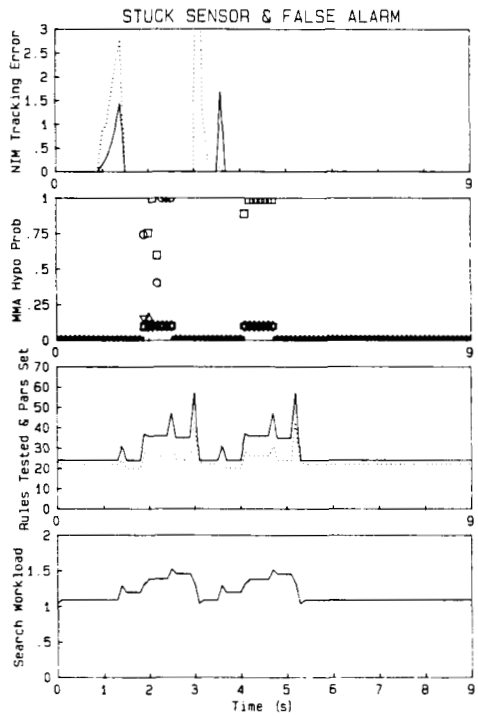

CONCLUSIONS

An expert systems approach to fault-tolerant flight control utilizing a rule-based backward-chaining search mechanism is an effective way to combine heuristic and analytical techniques. It allows the scheduling and selection of tasks to occur naturally within the action of rules, permits efficient flow of information between tasks, and allows the control system to be built incrementally.

Although at an early stage of development, the control system performs well and appears to provide an architecture suited to the difficult job of failure accommodation. The issues of failure diagnosis, parallel processing, and accommodation of additional failure modes are to be addressed next.

EXPERT SYSTEMS APPROACH ALLOWS

- NATURAL SCHEDULING AND SELECTION OF FAILURE-ACCOMMODATION TASKS
- EFFICIENT FLOW OF INFORMATION BETWEEN TASKS
- INCREMENTAL CONTROL SYSTEM GROWTH DURING DEVELOPMENT

EFFECTS OF JOINT RATE AND DISPLACEMENT CONSTRAINTS ON STABILITY REGIONS

P. C. Shrivastava
Department of Mechanical and Aerospace Engineering
Princeton University
Princeton, New Jersey

This block diagram shows the plant dynamics in normal mode coordinates, a linear feedback controller with command limits, and the actuator dynamics with rate and displacement limits. The objective is to examine the effects of joint rate and displacement saturation limits on the stability regions.

SCHEMATIC BLOCK-DIAGRAM

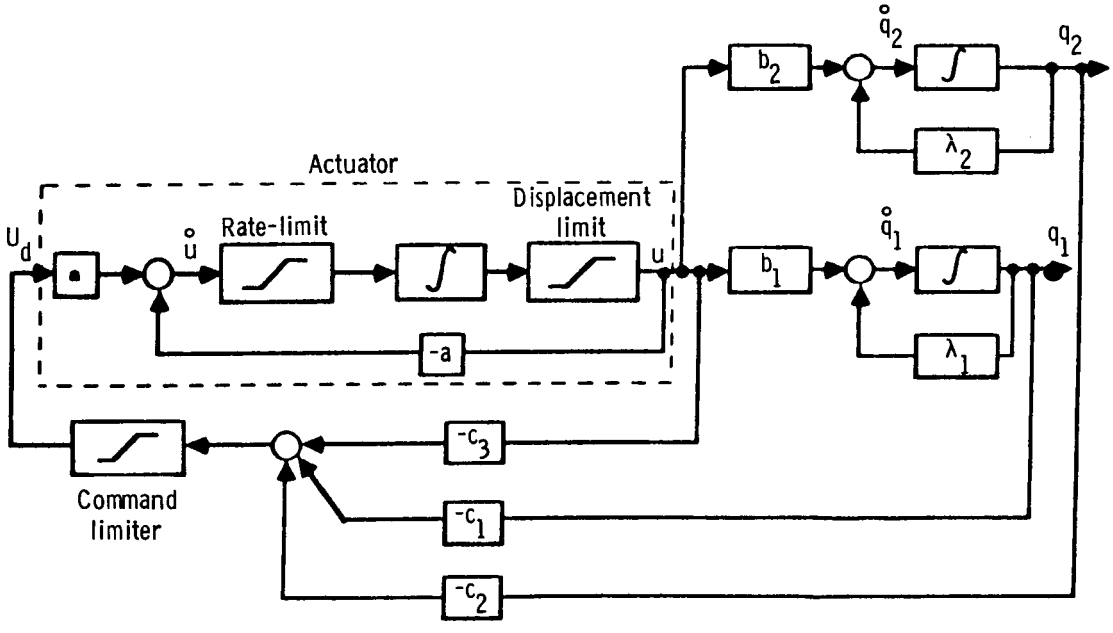

The unstable short-period dynamic model is transformed into normal mode coordinates, and it is augmented with actuator dynamics. The q mode is considered as the unstable mode. A linear feedback controller is used to provide closed-loop stability. We examine the stability boundaries with constrained actuator rate limits under varying bandwidth, displacement and command limits. The stability boundaries are unstable limit cycles in a phase-plane plot whose axes are the unstable mode and control deflection.

PROBLEM FORMULATION

- SHORT-PERIOD DYNAMICS

$$\dot{\alpha} = -L_\alpha \alpha + (1 - L_q/V_e)q$$

$$\dot{q} = M_\alpha \alpha + M_q q + M_{\delta e}\delta e$$

- ACTUATOR DYNAMICS

$$\dot{u} = -au + au_d$$

- AUGMENTED SYSTEM DYNAMICS (NORMAL MODE)

$$\begin{bmatrix} \dot{q}_1 \\ \dot{q}_2 \\ \dot{u} \end{bmatrix} = \begin{bmatrix} \lambda_1 & 0 & b_1 \\ 0 & \lambda_2 & b_2 \\ 0 & 0 & -a \end{bmatrix} \begin{bmatrix} q_1 \\ q_2 \\ u \end{bmatrix} + \begin{bmatrix} 0 \\ 0 \\ a \end{bmatrix} u_d$$

- LINEAR CONTROLLER

$$u_d = -c_1 q_1 - c_2 q_2 - c_3 u$$

The closed-loop stability by feedback of only the unstable mode requires the root magnitude to be greater than that of the unstable eigenvalues. In other words, the control bandwidth must be high enough to stabilize the system. This requirement is relaxed when the unstable mode and the control deflection are fed back because the effective actuator bandwidth is increased. Furthermore, feedback of control deflection also permits reduction in the feedback gain of the unstable mode.

CLOSED-LOOP DYNAMICS

- FEEDBACK OF UNSTABLE MODE (q_1 - MODE) [CONTROL LAW 1]
  - CHARACTERISTIC EQUATION:

$$(S - \lambda_2)\left[S^2 + (a - \lambda_1)\, S + (ab_1C_1 - a\lambda_1)\right] = 0$$

  - STABILITY CONDITIONS:

$$C_1 > \lambda_1/b_1$$

$$a > \lambda_1$$

- FEEDBACK OF UNSTABLE MODE AND CONTROL DEFLECTION (q_1 AND u) [CONTROL LAW 2]
  - CHARACTERISTIC EQUATION:

$$(S - \lambda_2)\left[S^2 + (a + aC_3 - \lambda_1)\, S + a(b_1C_1 - C_3\lambda_1 - \lambda_1)\right] = 0$$

  - STABILITY CONDITIONS

$$a(1 + C_3) > \lambda_1 \Rightarrow a > \frac{\lambda_1}{(1+C_3)}$$

$$b_1C_1 > \lambda_1(1 + C_3) \Rightarrow b_1C_1 > \lambda_1^2/a \qquad \text{SIGN OF } C_3?$$

The increase in the sizes of stability regions is not proportional to the bandwidth. At high bandwidths, the sizes of stability regions become almost independent of the bandwidth because the actuator is almost always rate-saturated. Feedback of control deflection permits increased region of rate-unsaturated operation due to reduced feedback gain requirement on the unstable mode. This helps increase the size of stability region size.

EFFECTS OF BANDWIDTH VARIATIONS (MCE GAIN)

CONTROL LAW 1

CONTROL LAW 2

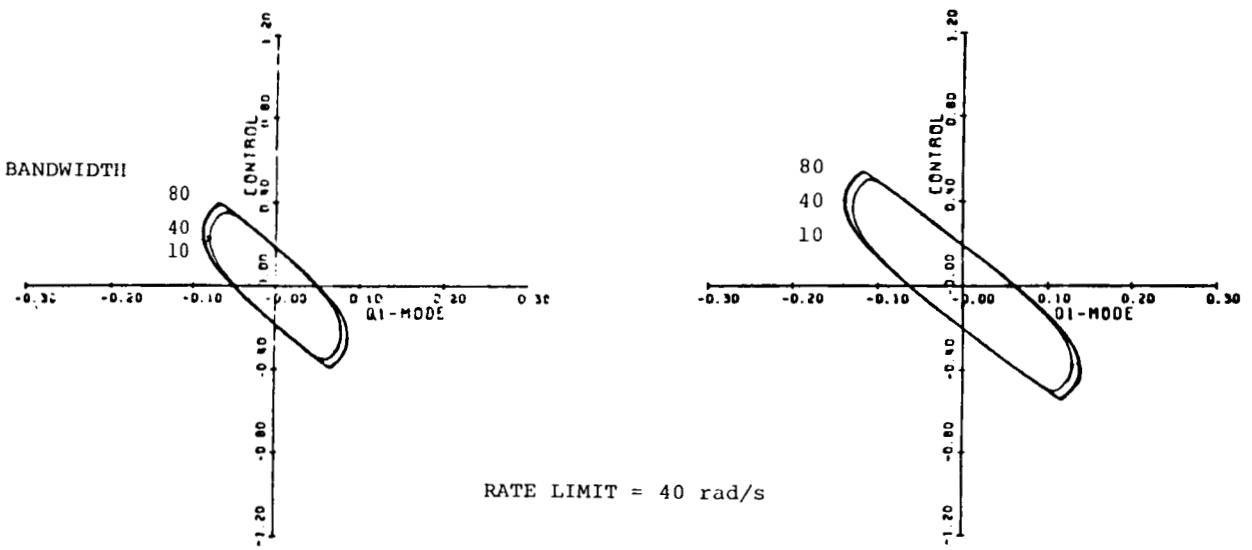

RATE LIMIT = 40 rad/s

While increase in the system feedback increases the closed-loop stability, it causes early rate saturation thereby reducing the sizes of stability regions.

EFFECTS OF BANDWIDTH VARIATIONS (TWICE MCE GAIN)

CONTROL LAW 1

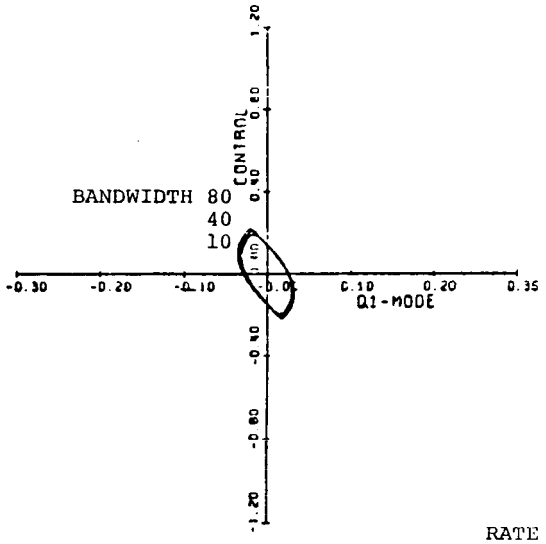

CONTROL LAW 2

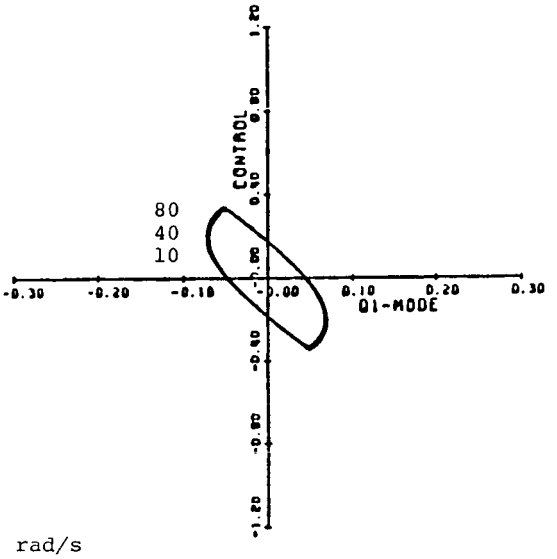

RATE LIMIT = 40 rad/s

Increasing rate limits implies relaxing the constraints, and the rate saturation occurs at relatively larger values of the control and state variables. Therefore, the stability region sizes increase with rate limits.

EFFECTS OF RATE-LIMIT VARIATIONS (MCE GAIN)

CONTROL LAW 1

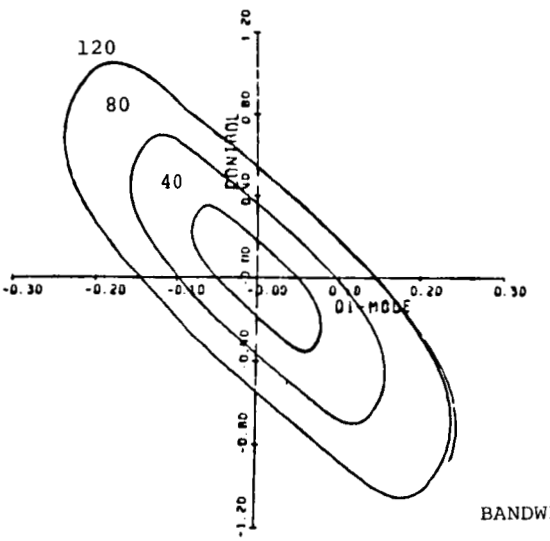

CONTROL LAW 2

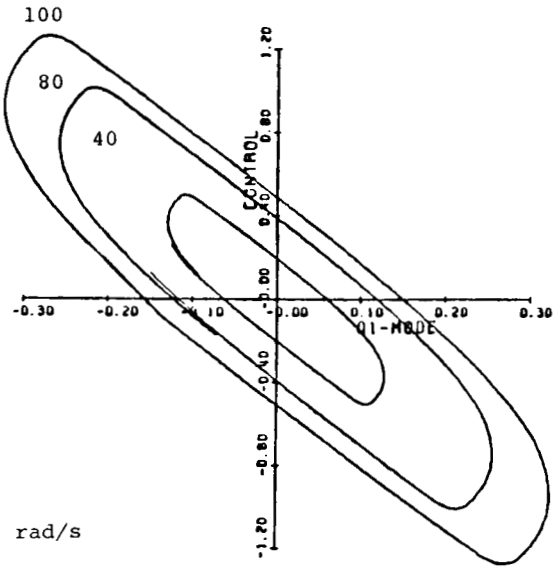

BANDWIDTH = 10 rad/s

Upon displacement saturation, the system is essentially open-loop and rate limit has no significance. The displacement limits restrain the area of closed-loop operation in the phase-plane, which causes drastic reduction in the sizes of stability regions. For this reason, the sizes of stability regions do not show significant size increases despite large increases in the rate limits.

EFFECTS OF IMPOSING DISPLACEMENT LIMIT (MCE GAIN)

CONTROL LAW 1

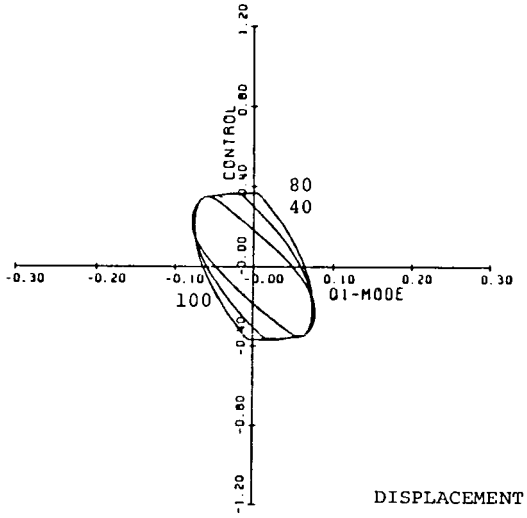

CONTROL LAW 2

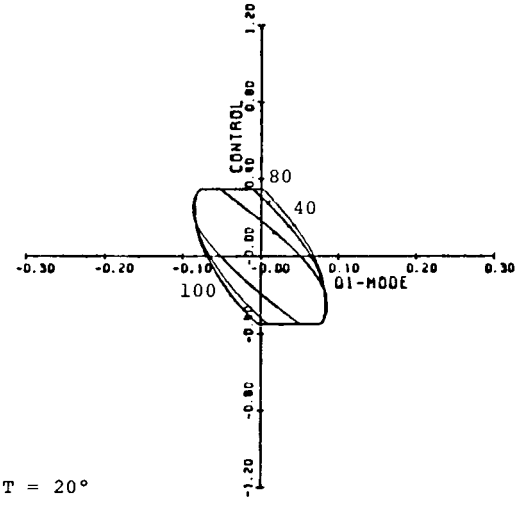

DISPLACEMENT LIMIT = 20°
BANDWIDTH = 10 rad/s

Marginal increases in the sizes of stability regions obtained for large increases in rate limits under displacement constraints suggest the possibility of invariance of stability regions with respect to the rate limits. Notice that a large part of the stability boundary lies within the rate-unsaturated region which is essentially sustained by the displacement limits. Increasing rate limits effectively bring in an even larger portion of the stability boundary within the rate-unsaturated region. Clearly, therefore there exists an upper bound on the rate limits beyond which the stability boundary is no longer influenced by the rate limits, as illustrated.

INVARIANCE OF STABILITY REGIONS WITH RATE LIMITS

(MCE GAIN CASE)

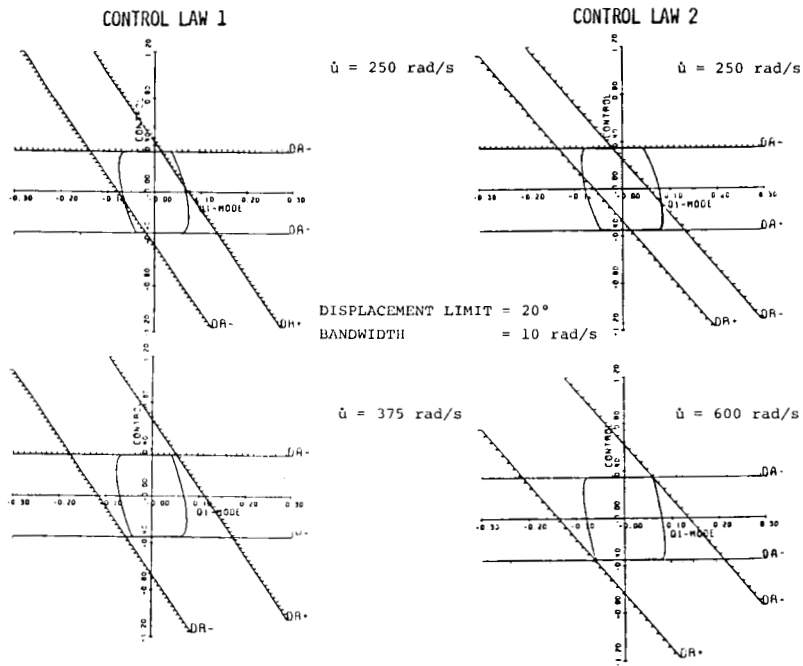

C-2

The large command limits do not affect the stability regions because the linear controller meets the demands required for closed-loop stability. Reduction in these limits deteriorates the controller capability. A small system divergence, due to the inability of the controller to meet the demanded control, causes a little expansion in the stability region; this divergence is overcome because of the reduced demand on the controller by a larger part of the stability boundary. As the command limit is reduced further, the system becomes unstable for relatively longer time placing even larger demands on the controller. The stability region vanishes because these demands cannot be satisfied by the controller.

EFFECTS OF COMMAND-LIMIT VARIATIONS (MCE GAIN)

CONTROL LAW 1

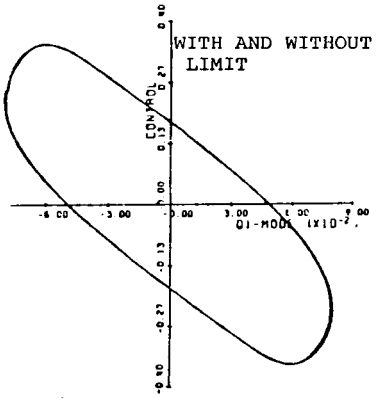

$|u_d|$ = 22 deg.

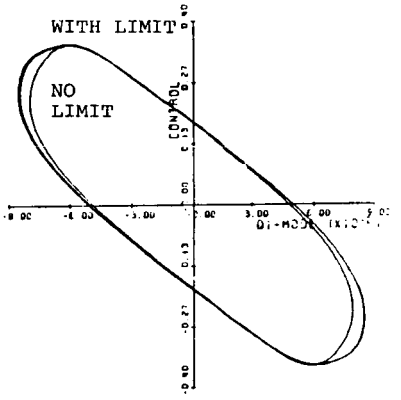

$|u_d|$ = 21 deg.

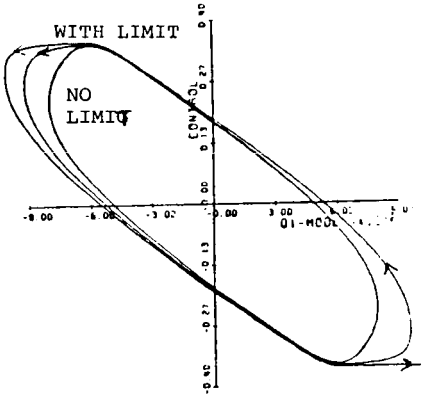

$|u_d|$ = 20.5 deg.

BANDWIDTH = 10 rad/s
RATE LIMIT = 40 rad/s

The limit cycle, representing the stability boundary in the phase-plane of unstable mode and control deflection, implies that a hypercylinder represents the overall stability region in the normal mode coordinates. With the state space coordinates located in the plane of normal modes, the stability regions clearly become functions of control deflection limits under rate constraints. Imposition of displacement limits implies that a chopped hypercylinder represents the stability region. Therefore, finite stability regions can exist in the state space coordinates only for those controls that satisfy the displacement saturation constraints.

INTERPRETATION OF RESULTS IN PHYSICAL COORDINATES

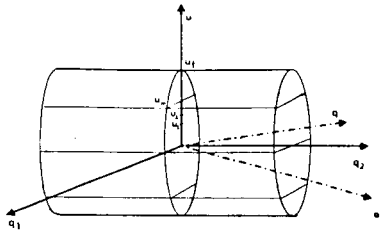

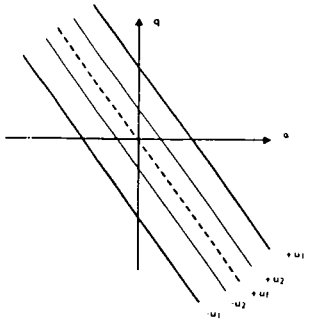

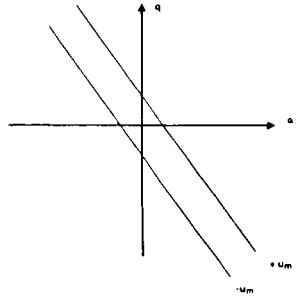

Under rate constraints, a hypercylinder is shown to represent the stability region in the normal mode coordinates when a saddle-point type system is controlled by feedback of the unstable mode and control deflection. Its intersection with the plane of unstable mode and control deflection is an unstable limit cycle. An increase in rate limits results in increased size of the stability regions, but imposing displacement constraints causes drastic reduction in their sizes. That is, the stability regions are largely dependent upon the displacement limits, and they can even be made independent of the rate limits. Feedback of control deflection effectively increases the region of rate-unsaturated operation resulting in increased sizes of stability regions. However, the sizes of stability regions are reduced with increased feedback gain due to early rate saturation. Unlike the case of joint rate and displacement constraints where the existence of a stability region is always guaranteed, in the case of joint rate and command constraints, the stability region can disappear when the command limit is reduced below a certain limit.

CONCLUSIONS

- LIMIT CYCLE REPRESENTS STABILITY BOUNDARY
- MARGINAL EFFECT OF ACTUATOR BANDWIDTH
- INCREASE IN STABILITY REGION SIZE WITH RATE LIMITS
- SIGNIFICANT SIZE REDUCTION UNDER CONSTRAINED DEFLECTION
- LARGER REGION WITH FEEDBACK OF CONTROL DEFLECTION
- REDUCED SIZES WITH INCREASED GAIN
- INTOLERANCE OF STABILITY REGIONS TO COMMAND LIMITS

AN EXPERT SYSTEM FOR AIR TRAFFIC CONTROL SYSTEM

Takashi Sensui
Department of Mechanical and Aerospace Engineering
Princeton University
Princeton, NJ

The objective of this project is to design a control logic which automates all or parts of the guidance function of air traffic control systems. A particular interest has been focused on automation of the terminal area control system, and preliminary study has been done on development of an expert system: a computer system that is capable of producing similar commands to those normally given by human controllers in various situations. The system may be used to assist controllers by providing them with feasible options in guiding each aircraft in the control area to its desired destination. It is assumed, however, that the final decision is still made by the controller and the computer system is used only as a supporting facility to increase efficiency and safety of the system.

AN EXPERT SYSTEM FOR AIR TRAFFIC CONTROL

* General Procedures for Terminal Area Control
* Previous Works on Automation of Terminal Area Control
* Expert Systems
* PROLOG; Artificial Intelligence Programming Language
* Conclusion and Plans for Further Study

Generally, a terminal control area consists of a designated runway, an outer marker, outer fixes, and nominal paths connecting outer fixes with the outer marker. The primary function of a TCA controller is to safely direct each arriving aircraft from one of the outer fixes to the outer marker. Aircraft are then handed over to the tower controller for the final approach. If an aircraft is too close to another aircraft, i.e. a conflict is being predicted, the controller has to direct one of the aircraft into a delay maneuver or a holding pattern.

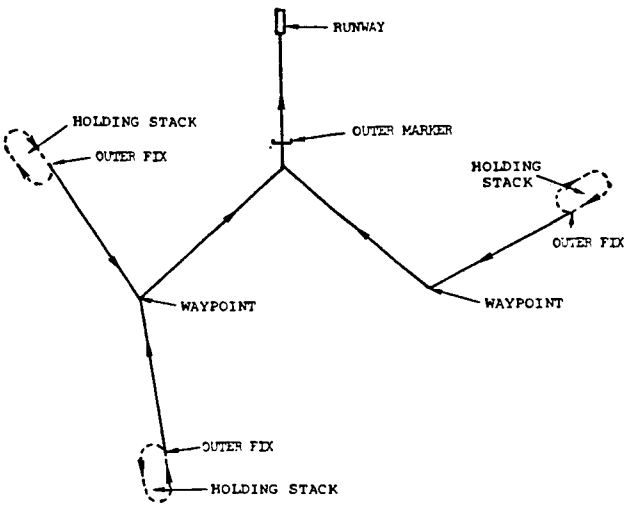

A TYPICAL TERMINAL CONTROL AREA

In an effort to automate the guidance process, Athans at MIT used a quadratic optimizing cost function to decide which aircraft is to leave the nominal path and go into a delay maneuver.[1] The algorithm assumes that desired separations are known and there is a unique desired speed. Penalty functions are included in the cost function so that any deviation from these desired values causes a higher cost. Aircraft with higher cost values are usually directed into delay maneuvers if conflicts are probable.

Erwin at Boeing Airplane Co. has proposed a new method called strategic control method which uses parallel paths to solve conflicts instead of delay maneuvers.[2] In this method, the terminal control area is extended from the usual 30 nautical-mile-radius to approximately 150 nautical-mile-radius, and the sequencing of arriving aircraft is done by the computer during the descent from cruise altitudes prior to the initial approach. He claims that the strategic control method will achieve an increased system capacity as well as a significant fuel savings.

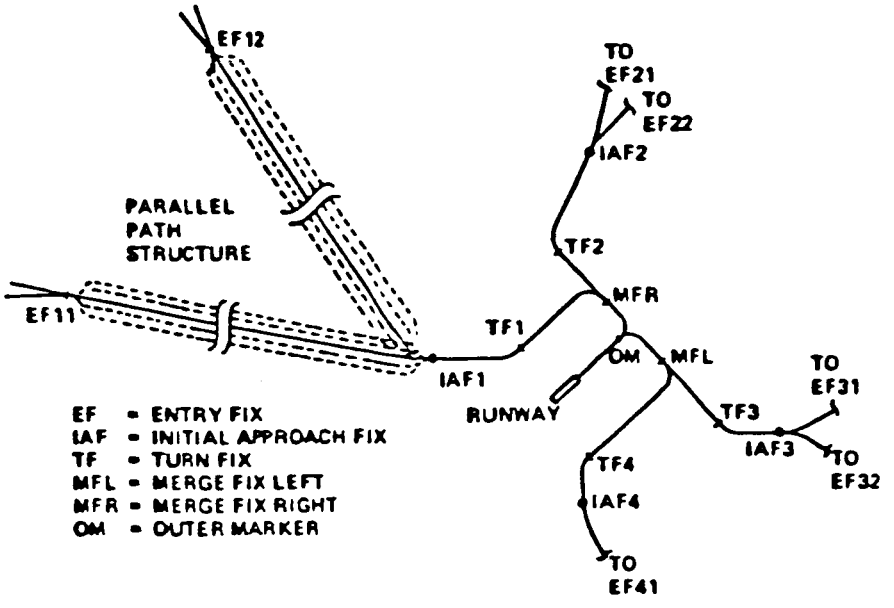

STRATEGIC CONTROL METHOD LAYOUT

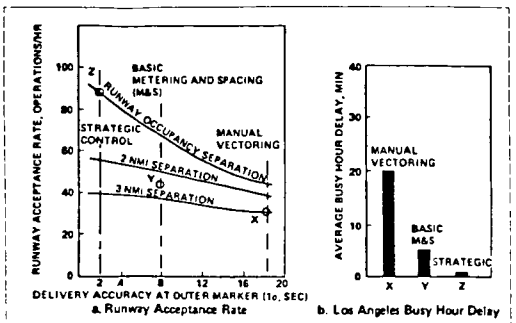

INCREASED CAPACITY WITH STRATEGIC CONTROL

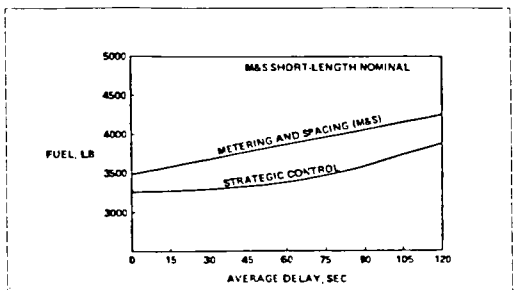

FUEL SAVINGS WITH STRATEGIC CONTROL

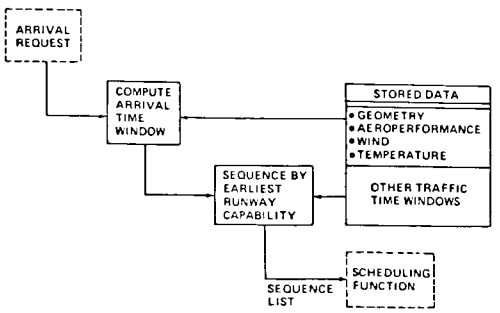

SEQUENCE DETERMINATION

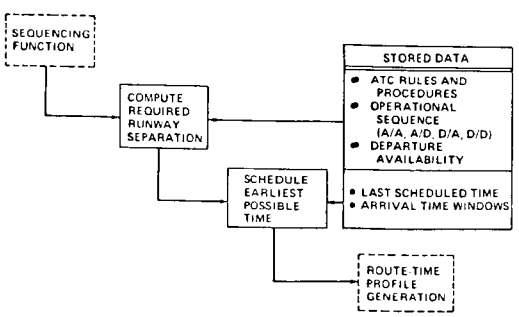

SCHEDULE DETERMINATION

The main problems in implementing these automatic systems are data management and the man-machine interface. First, the automated system has to consider various types of data, such as geometry of the controlled air space, aeroperformance of each aircraft, weather conditions, etc., in its calculations, so it must store enormous amounts of data. It must also be able to find any data in a relatively short period of time. Second, the automated system has to be able to "communicate" with controllers or pilots in order to make suggestions or to answer questions.

It is rather difficult to solve these problems with a conventional computer system, and application of artificial intelligence seems appropriate. Particularly, an expert system may be used as an interface between a human controller and a computer. An expert system is a software system which encapsulates specialist knowledge about a specific area of expertise and is capable of making intelligent decisions within that area. It can interpret the stream of numbers generated by the computer and present them in a more easily understood manner.

In continuing this project, the next step is to define a set of rules that constructs the knowledge base of the expert system. These rules will be encoded from manuals and from conversation with controllers, and they should cover all possible situations. Then the expert system, its control logic and knowledge base, will be programmed in PROLOG: an artificial intelligence programming language.

REFERENCES

1. Athans, M., "An Approach to Semiautomated Optimal Scheduling and Holding Strategies for Air Traffic Control," JACC Paper No. 6-D6, Washington University, St. Louis, MO, August 1971.

2. Erwin, Ralph L., Jr., "Strategic Control of Terminal Area Traffic", Plans and Developments for Air Traffic Systems, AGARD Conference Proceedings No.188, May 1975.

Standard Bibliographic Page

1. Report No.	2. Government Accession No.	3. Recipient's Catalog No.
NASA CP-2453		

4. Title and Subtitle	5. Report Date
Joint University Program for Air Transportation Research - 1985	July 1987
	6. Performing Organization Code
7. Author(s)	8. Performing Organization Report No.
Frederick R. Morrell, Compiler	L-16256
9. Performing Organization Name and Address	10. Work Unit No.
NASA Langley Research Center Hampton, VA 23665-5225	505-66-01-07
	11. Contract or Grant No.
12. Sponsoring Agency Name and Address	13. Type of Report and Period Covered
National Aeronautics and Space Administration Washington, DC 20546-0001	Conference Publication
	14. Sponsoring Agency Code

15. Supplementary Notes

16. Abstract

This report summarizes the research conducted during 1985 under the NASA/FAA sponsored Joint University Program for Air Transportation Research. The material was presented at a meeting held at the Federal Aviation Administration Technical Center, Atlantic City, New Jersey, January 30, 1986. The Joint University Program is a coordinated set of three grants sponsored by NASA Langley Research Center and the Federal Aviation Administration, one each with the Massachusetts Institute of Technology, Ohio University, and Princeton University. Completed works, status reports, and bibliographies are presented for research topics, which include navigation, guidance, control, and display concepts. An overview of the years activities is also presented.

17. Key Words (Suggested by Authors(s))	18. Distribution Statement
Avionics Low-frequency terrestrial navigation Aircraft guidance navigation and control	Unclassified - Unlimited Subject Category 01

19. Security Classif.(of this report)	20. Security Classif.(of this page)	21. No. of Pages	22. Price
Unclassified	Unclassified	106	A06

For sale by the National Technical Information Service, Springfield, Virginia 22161